resources

MDPI

Article

Critical Raw Materials Supply: Challenges and Potentialities to Exploit Rare Earth Elements from Siliceous Stones and Extractive Waste

Xinyuan Zhao [1,2], Faten Khelifi [3], Marco Casale [4,*], Alessandro Cavallo [5], Elio Padoan [3], Ke Yang [1] and Giovanna Antonella Dino [6]

1 School of Mining Engineering, Anhui University of Science and Technology, Huainan 232001, China
2 School of Mining and Geomatics Engineering, Hebei University of Engineering, Handan 056006, China
3 Department of Agricultural, Forest and Food Sciences (DISAFA), University of Turin, 10095 Grugliasco, Italy
4 Department of Management, University of Turin, 10134 Turin, Italy
5 Department of Earth and Environmental Sciences, University of Milano-Bicocca, 20126 Milan, Italy
6 Earth Sciences Department, University of Turin, 10125 Turin, Italy
* Correspondence: ma.casale@unito.it

Abstract: Critical raw materials (CRMs) supply is a challenge that EU countries have to face, with many thinking about domestic procurement from natural ore deposits and anthropogenic deposits (landfills and extractive waste facilities). The present research focuses on the possibilities linked to the supply of CRMs and the potential for exploiting rare earth elements (REEs), investigating a large variety of extractive waste and siliceous rocks in the Piedmont region (Northern Italy). Indeed, the recovery of REEs from the extractive waste (EW) of siliceous quarries and other siliceous ore deposits can be a valuable way to reduce supply chain risks. Starting with a review of the literature on mining activities in Piedmont and continuing with the sampling and geochemical, mineralogical, petrographic, and environmental characterization of EW facilities connected to siliceous dimension stones, of kaolinitic gneiss ore deposits, and of soils present near the investigated areas, this study shows that the degree of REEs enrichment differs depending on the sampling area (soil or EW) and lithology. The concentration of REEs in the EW at some sampling sites fulfils the indicators of industrial-grade and industrial recovery; the high cumulative production and potential market values of EW and the positive recovery effects through proven methodologies indicate a viable prospect of REE recovery from EW. However, REE recovery industrialization faces challenges such as the difficulty in achieving efficient large-scale recovery due to large regional differences in REE abundance, the mismatch between potential market value and waste annual production, etc. Nonetheless, in the future, EW from dimension stone quarries could be differentially studied and reused based on the enrichment and distribution characteristics of trace elements. The present paper shows investigation procedures undertaken to determine both CRMs potentialities and environmental issues (on the basis of literature data employed to select the more-promising areas and on sampling and characterization activities in the selected areas), together with procedures to determine the waste quantities and tentative economic values of REEs present in the investigated areas. This approach, tested on a large area (Piedmont region), is replicable and applicable to other similar case studies (at EU and non-EU levels) and offers decision makers the possibility to acquire a general overview of the potential available resources in order to decide whether and where to concentrate efforts (including economic ones) in a more detailed study to evaluate the exploitable anthropogenic deposits.

Keywords: rare earth elements; critical raw materials; geochemistry characterization; circular economy; extractive waste

Citation: Zhao, X.; Khelifi, F.; Casale, M.; Cavallo, A.; Padoan, E.; Yang, K.; Dino, G.A. Critical Raw Materials Supply: Challenges and Potentialities to Exploit Rare Earth Elements from Siliceous Stones and Extractive Waste. *Resources* **2024**, *13*, 97. https://doi.org/10.3390/resources13070097

Academic Editor: Angel F. Mohedano

Received: 15 May 2024
Revised: 5 July 2024
Accepted: 9 July 2024
Published: 15 July 2024

1. Introduction

Rare earth elements (REEs) are used in many important fields connected to energy and ecological transition (such as solar cells [1], wind turbines [2], and new energy vehicles [3])

and represent a great share of the EU's economic growth and competitiveness enhancement [4]. Due to the high demand and the heavy dependence on imports, engendering high-risk situations such as geopolitical conflicts and resource monopolies [5], REEs are listed in Europe as critical raw materials (CRMs), together with other 33 commodities. Europe has been taking measures to eliminate its dependence on third-party countries for CRMs, such as via the "Critical Raw Materials Act (2023)", which sets goals for the domestic procurement (from natural and anthropogenic deposits), processing, and recovery of CRMs from waste recycling, together with other actions more connected to political and strategical agreements with third countries [6,7].

Commodities coming from waste recovery and recycling (circular economy approach) are not enough to guarantee the needed raw materials (RM) and CRM supply; thus, mining and quarrying activities remain the first activities with which to exploit resources fundamental to guaranteeing EU development. Mining and quarrying are accompanied by the generation of extractive waste (EW), which, for a long time, has been stocked in uncontrolled sites, exposed to erosion and weathering processes, and causing potentially severe risks to the environment and humans [8–10]. In the European Alps and worldwide, many active or abandoned mining and quarrying sites have left behind large amounts of EW, often not rehabilitated. On the one hand, EW fine particles could be easily transported by weathering and precipitation, could settle on surfaces, and could become components of surface soils [11–13]. Thus, soils near extractive areas are likely to be affected by quarrying and mining activities. On the other hand, EW exploitation can positively contribute to guaranteeing RM and CRM supply, simultaneously reducing the potential environmental impacts associated with EW facilities. The potential RM/CRM recovery from EW facilities and the potential environmental impacts associated with EW facilities were analyzed in this study.

Several recent studies have investigated the presence of REEs in EW connected to Italian siliceous rocks (granite, gneisses, kaolinitic sands) [14–16] and shown that they enclose interesting contents of REEs ore minerals (e.g., monazite and allanite). These make these rocks potential resources for the recovery and extraction of REEs.

In some cases, part of the EW is currently being exploited for ceramic production (after mineral processing to separate femic minerals not appropriate for ceramic products). If the REEs content is estimated as "worth being exploited", joint exploitation for raw materials (RMs) (for ceramic) and CRMs (REE minerals associated with femic minerals in siliceous rocks) could be planned.

There have been cases of REEs recovery from various mining solid wastes, such as tailings [17], waste rocks from the carbonatites [18], and mining residual sludge [19], etc. However, there is currently a lack of studies that comprehensively assess the industrial potential and value of REEs recovery from EWs associated with dimension stones and siliceous rocks at large in the European Alps. The potential and challenges of REEs recovery from siliceous rock waste are currently unknown.

The present paper, which shows investigation procedures undertaken to determine both CRMs potentialities and environmental issues (on the basis of literature data employed to select the more promising areas and the sampling and characterization activities in the selected areas), together with procedures to determine the waste quantities and tentative economic values of CRMs present in the investigated areas, focuses on siliceous rocks, EW facilities, and kaolinitic gneiss ore deposits present in the Piemonte region (Northern Italy).

In particular, starting from the investigation and characterization of a wide potential anthropogenic deposit (intended as "EW facilities") connected to siliceous dimension stone wastes produced at the Piedmont level—as well as of ore deposits for kaolinitic gneiss exploitation (associated with waste EW deposits of quartzite)—to determine challenges and potentialities for the exploitation of REEs from silicate rocks, the aim of this paper is to evidence where major concentrations of REEs are present and where the amounts of exploitable materials can guarantee an adequate quantity to be processed. The approach applied in this study can be replicated in other research areas characterized by the presence

of siliceous dimension stones (and consequently EW facilities) and/or by the presence of kaolinitic sands and gneisses.

In this context, this paper focuses on the connections between EW facilities and soils. In areas where EW facilities are not known or are no longer visible, as in rehabilitated quarry dumps, the presence of REEs in soils could be useful in defining the areas potentially of interest due to the presence of rehabilitated EW facilities. Furthermore, the characterization of soils is also aimed at the investigation of potential emerging pollutants.

In detail, mineralogical, petrographic, geochemical, and environmental characterization of the EWs (granite, gneiss, diorite, and quartzite), kaolinitic gneiss deposits, and soils near quarries in the Northwest Italy region were carried out. The potential connection between soil and EW was revealed based on the presence of trace elements (mainly potentially toxic elements: CRM and REE); then, the industrial potential and challenges of REEs recovery from quarry EW were studied, and future work was prospected.

2. Materials and Methods

2.1. Investigation and Description of Sampling Area

Northwestern Italy, and the Piedmont Region in particular, is characterized by a wide presence of dimension stones (igneous, metamorphic, and sedimentary). Different EWs in four quarrying areas (Figure 1), linked to specific dimension stones, were investigated. A brief description of the four quarrying sites (Luserna Stone quarry basin, the VCO quarrying area [15,20], the Traversella quarry area [21,22], and the Monte Bracco quarrying and mining area [20,23]) follows.

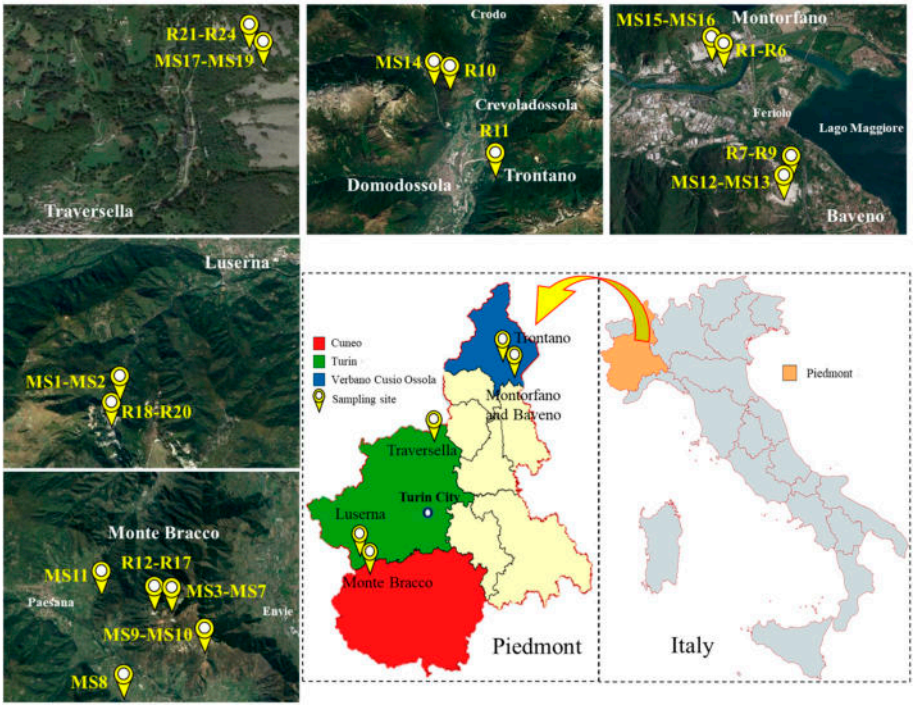

Figure 1. Sampling location.

The Luserna Stone quarry basin is located on the border of Cuneo and Torino and has 72 active quarries (data from 2017 census), mainly mining Luserna Stone, a lower Permian leucogranitic orthogneiss pertaining to the Dora Maira Massif, which outcrops in a quite-large area in the Cottian Alps.

The VCO quarrying area, close to the border with Switzerland, shows 36 authorized quarries (data from 2017 census). The investigated EW are related to White Montorfano and Pink Baveno granites and Serizzi and Beole gneisses (a heterogeneous group of orthogneisses, with relatively similar mineralogical compositions but different textures and

microstructures). Two processing plants that treat granite EW are present in the area and produce a quartz–feldspar concentrate for the ceramic industry and several by-products (rich in Fe minerals) for building and environmental purposes.

Traversella diorite quarries (3 active quarries in 2017) are located nearly 60 km north of Torino; the Traversella area is characterized by a very important but no longer operating mining district for iron exploitation (from the only exploited skarn-type mineralization in the Alps present at the point of contact between a dioritic body and the pre-existing host rocks).

Finally, the Monte Bracco area is located in the Dora Maira Massif; it is represented by an isolated relief, north–south elongated, and mainly formed by phengite-bearing orthogneisses, paragneisses, and some lenses of quartzite that crop out in the uppermost part of the mount. At the southern of Monte Bracco (Tre Fontane quarry and other regions), a deep clayey alteration ("kaolinization") of the gneisses occurs.

2.2. Sampling Criteria

Sampling location and specific information on sampled EW, kaolinitic gneisses (from Monte Bracco), and soil are shown in Table 1 and Figure 1. The sampling activities of EWs took place in both abandoned and active quarries (Serizzi and Beole gneisses, Montorfano and Baveno granites, Traversella diorite, Bargiolina quartzite, and kaolinitic gneiss from Monte Bracco, Luserna Stone gneiss) and stone processing plants for granite quarry waste exploitation present in VCO quarry areas. To obtain representative samples of each solid waste pile, a systematic sampling strategy was adopted [24]. Each solid waste dump was sampled at an interval of 5 m to cover the entire sampling site (producing representative samples for each investigated area). The field sampling process for the fine-sized and coarse samples is shown in Figure 2a.

Table 1. Sampling information.

EW No.	EW Lithotype and Size	Quarrying Area	Soil No.
R1	Granite waste (0–60 mm)	Montorfano, VCO	MS15 MS16
R2	Granite waste (60–300 mm)	Montorfano, VCO	
R3	From granite processing (not magnetic concentrate)	Montorfano, VCO	
R4	From granite processing (magnetic concentrate—sand)	Montorfano, VCO	
R5	From granite processing (magnetic concentrate—fine)	Montorfano, VCO	
R6	From granite processing (not magnetic concentrate)	Montorfano, VCO	
R7	Granite waste, coarse	Baveno, VCO	MS12 MS13
R8	From granite processing (powder fraction)	Baveno, VCO	
R9	From granite processing (magnetic concentrate)	Baveno, VCO	
R10	Gneiss waste, coarse	Crevoladossola, VCO	MS14
R11	Residual sludge from gneiss	Trontano, VCO	-
R12	Kaolinitic sand, fine	Monte Bracco	MS3 to MS11
R13	Kaolinitic sand, fine	Monte Bracco	
R14	Kaolinitic sand, fine	Monte Bracco	
R15	Kaolinitic sand, fine	Monte Bracco	
R16	Kaolinitic sand (brown), fine	Monte Bracco	
R17	Quartzite waste, coarse	Monte Bracco	
R18	Gneiss waste, coarse	Rorà, Luserna	MS1 MS2
R19	Gneiss waste, coarse	Rorà, Luserna	
R20	Gneiss waste, coarse	Rorà, Luserna	
R21	Diorite waste, coarse	Traversella	MS17 MS18 MS19
R22	Diorite waste, coarse	Traversella	
R23	Joint filling in diorite, brown fine fraction	Traversella	
R24	Filled clasts in Diorite joint, brown coarse fraction	Traversella	

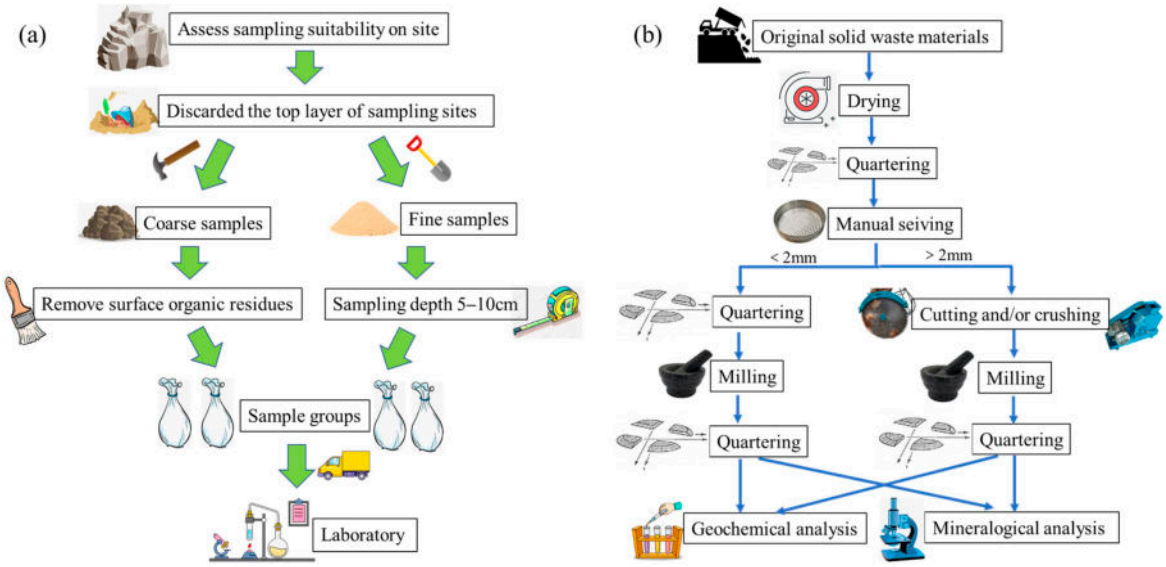

Figure 2. Procedures for field sampling (**a**) and sample preparation in the laboratory (**b**).

The sampling activities of the soil were performed in proximity of the quarrying zones and /or the EW facilities. To this end, 19 topsoil samples (depth 0–20 cm) were collected in the four investigated areas; the number of sites for each area was chosen according to the number of waste areas and their variability. Each sample consists of 5 subsamples collected at one meter from another.

Laboratory activities included the drying, sieving, quartering [25], grinding, and testing of all samples. For each sampling site, a representative sample was stored for backup [26]. The preparation process of samples and sub-samples in the laboratory is shown in Figure 2b.

2.3. Materials Characterization

2.3.1. Mineralogy and Petrology

Rock samples were characterized for mineralogy and petrography via the combined use of polarized light microscopy (PLM) on thin sections and X-ray powder diffraction (XRPD); soil samples were investigated only via XRPD. Rock fragments were cut by a diamond disk cutter to obtain the thin sections for PLM analysis. The mineral chemistry of REE-bearing phases was preliminary assessed by SEM in combination with an EDS analyzer on carbon coated samples. The instruments, methods, and parameters used in PLM, XRPD, and SEM + EDS analysis can be found in previously published references [15,20].

2.3.2. Geochemistry

Rock and soil samples were characterized geochemically for their total (rocks) or aqua regia (soils) content of inorganic elements, including REEs and potentially toxic elements. EW and natural ore (kaolinitic gneisses) samples were digested using a four-acid digestion (HF, HCl, HNO_3, $HClO_4$); thus, the samples were digested first by hydrofluoric acid, then by a mixture of nitric and perchloric acids, and then heated using a high-precision temperature control system in numerous ramping and holding cycles until dry. After drying, samples were brought back to solution with hydrochloric and nitric acids, while the soil samples underwent a pseudo-total digestion. Thus, an amount of 0.5 g of soil was digested using Aqua regia inside a microprocessor-controlled digestion block. The samples were diluted and analyzed using ICP-MS and ICP-OES techniques from an accredited laboratory (Actlabs LTd., Ontario, Canada). Quality insurance methods used duplicate analyses and different certificate reference materials (OREAS 47, OREAS 45d, OREAS 907).

Based on trace element test results, the upper continental crust (UCC) (Wedepohl 1995) was used as a reference by which to normalize the CRM and REE abundances of soil and rock samples from each sampling site. The geochemical characteristic parameters of REEs, such as δEu, δCe, (La/Yb)N, (La/Sm)N, (Gd/Lu)N, and ∑LREE/∑HREE, were calculated using chondrite normalization (Boynton 1984). The calculation methods of δEu and δCe are as shown in Equations (A1) and (A2) in the Appendix A. (La/Yb)N, (La/Sm)N, and (Gd/Lu)N are the ratios of La and Yb, La and Sm, and Gd and Lu, respectively, after chondrite normalization [27–29].

2.3.3. Environmental Risk

Based on the trace element results, the potential environmental risks of soil and EW were comprehensively evaluated. The characterization indicators include the geoaccumulation index (GI), the pollution load index (PLI), the ecological harm coefficient (EHC), the human health risk index with non-carcinogenic (HI), and the carcinogenic risk index (CR) [30–32]. The calculation methods, meanings, and values of each index are shown in Equations (A3)–(A10) and Tables A1 and A2 (Appendix A). Among them, GI and PLI are only calculated for soil. Since the quarry is far away from residential areas, only the health risks of adult workers in the quarry were assessed, assuming that adult workers would work in the quarry for 250 days per year and for 30 years during their lifetime. Due to the lack of carcinogenic slope factors, only the carcinogenic risks of individual metals under different intake pathways were evaluated. The reference value of a metal element i refers to the average metal concentration of natural topsoil in the Piedmont region [33]. Due to the lack of reference concentration of the As element, only the GI, PLI, and EHC of Cr, Cu, Zn, Cd, Pb, and Ni elements in the soil were calculated. The reference value of metal element i in EW refers to the continental crustal abundance [34]. The Cd elemental concentration is lower than the instrument detection limit of 0.3 ppm; so, a value of 0.2 ppm is used for estimation.

3. Results and Discussion

3.1. Mineralogical and Petrographical Characterisation

The results of the mineralogical analysis via XRPD are shown in Figure 3 for rock and soil samples, respectively. Considering the nature of the materials, a composition of only crystalline phases is assumed (there is no evidence of the presence of amorphous/glassy phases). Figure 4 shows SEM back-scattered electrons image with the EDS spectrum of some EW samples.

Granite EW (R1–R9) are composed mainly of quartz, K-feldspar (orthoclase and microcline), plagioclase (oligoclase), and smaller amounts of biotite (frequently altered in chlorite). Typical accessory minerals are zircon, apatite, monazite (REE-rich mineral), and opaques (pyrite, Fe oxides, arsenopyrite). Similarly, the orthogneisses EW (Beola and Serizzo) are composed of quartz–feldspar. However, compared to the granites, the proportions of K-feldspar and plagioclase changed, and greater amounts of white mica and biotite (R10 and R11) are present. Subordinate amounts of chlorite and allanite, an REE-rich variety of epidote, are present in gneisses; accessory minerals are the same as granite rocks. The kaolinized gneiss in Monte Bracco also derive from quartz–feldspathic protoliths, but they contain variable (sometimes appreciable) amounts of kaolinite and/or illite and a lack of biotite. Accessory minerals are apatite, zircon, and xenotime. In contrast, diorite EW are basic rocks with significantly reduced quartz content, composed mainly of plagioclase (andesine to oligoclase), amphibole (hornblende, sometimes partially altered into tremolite-actinolite), biotite (partially chloritized), and sometimes small amounts of pyroxene (clinopyroxene). Accessory minerals are apatite, zircon, titanite, opaques (oxides and sulphides), and trace amounts of monazite. They are medium-to-fine-grained, generally homogeneous, with massive texture, sometimes slightly foliated.

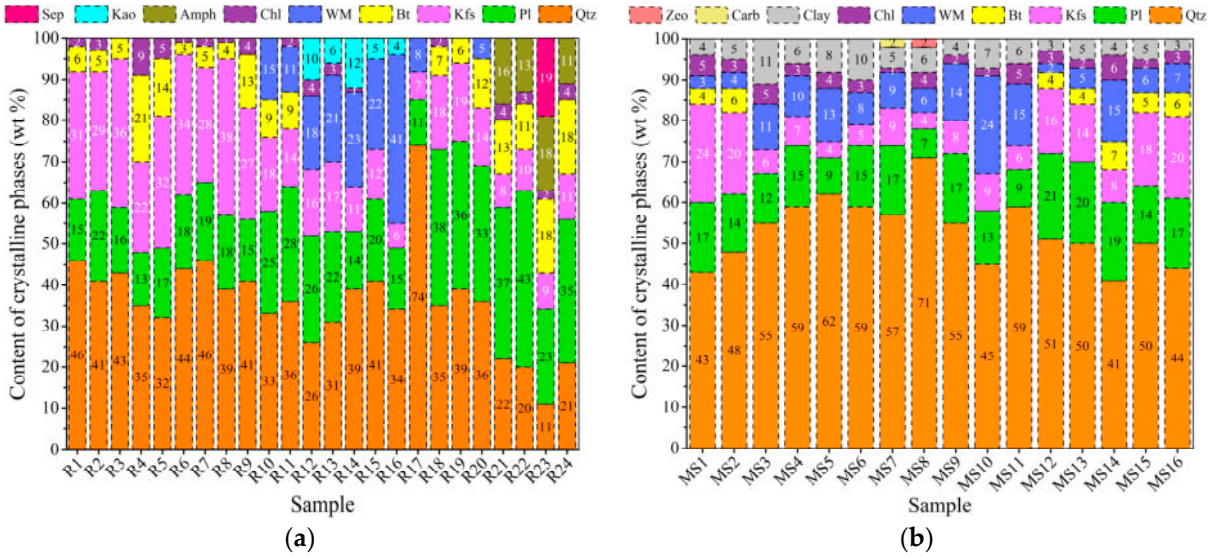

Figure 3. Main minerals present in soil and EW samples: (**a**) EWl; (**b**) soil. Qtz = quartz; Pl = plagioclase; Kfs = K-feldspar; Bt = biotite; WM = white mica (muscovite)—illite; Chl = chlorite; Amph = amphibole (mainly hornblende); Clay = illite, kaolinite, mixed clays; Carb = carbonates (calcite); Zeo = zeolites; Kao = kaolinite; Sep = sepiolite; Amph = amphibole (mainly hornblende). Some mineral contents are lower than limit of detection and are ignored here.

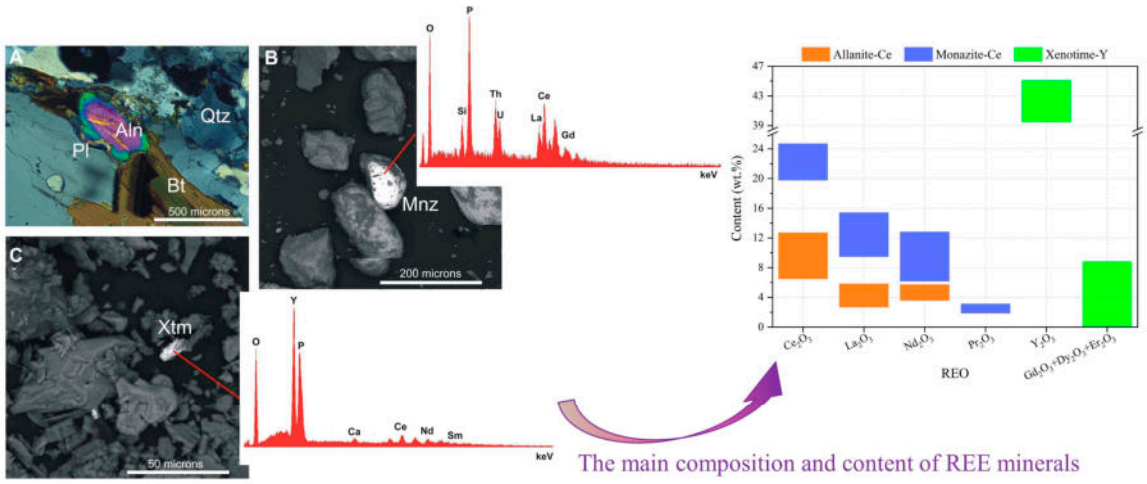

Figure 4. PLM micrograph (**A**) and SEM back-scattered electrons images with EDS spectrum of EW (**B**,**C**): (**A**) allanite (Aln) crystal of a Serizzo Antigorio gneiss sample, PLM micrograph, and crossed polars; (**B**) SEM back-scattered electrons image of a monazite-Ce (Mnz) crystal of a Baveno granite sample; (**C**) SEM back-scattered electrons image of a Xenotime-Y (Xtm) crystal of a kaolinitic sand sample from Monte Bracco.

The soil samples basically reflect the nature of the underlying bedrock. However, in addition to the abundance of quartz, plagioclase, K-feldspar, and white mica, varying amounts (3–11 wt.%) of clay minerals (e.g., illite, kaolinite, and mixed clays) are present in soil, depending on pedogenesis. In some cases, small amounts or traces of accessory and/or secondary minerals are present in soil, such as carbonates (sample MS7), zeolites (sample MS8), and clay minerals.

As for REE minerals (Figure 4), traces of minerals resistant to meteoric alteration were found, mainly monazite, in the EW and soils, with lesser amounts or traces of xenotime-Y. A special case is represented by Monte Bracco, where appreciable amounts of xenotime-Y are present, and where REEs are sometimes concentrated by clay minerals (mainly on illite and

kaolinite) [35]. Allanite-Ce is an REE-bearing variety of epidotes, which is quite common especially in the "Serizzo" and "Beola" gneisses, whose components are Ce_2O_3, La_2O_3, Nd_2O_3, and traces of Y_2O_3, Pr_2O_3, and Sm_2O_3. Monazite-Ce is the most common REE mineral in granites and diorites, with its main composition being similar to Allanite-Ce and a small amount of Pr_2O_3. ThO_2 and U_3O_8 are also present, with 8.7 wt.% and 1.5 wt.%, respectively. Xenotime-Y is quite common, especially in the Monte Bracco samples, where the main component is Y_2O_3, as well as traces of Gd_2O_3, Dy_2O_3, and Er_2O_3 (up to 8.8 wt.%); this area is also characterized by light rare earth element (LREE)-enriched clay minerals, especially illite and kaolinite.

In summary, mineralogical and petrographic analyses showed the presence of valuable REE minerals (monazite and allanite), with mineral–chemical, dimensional, and textural characteristics suitable for possible exploitation, albeit with different characteristics depending on locations and lithologies.

3.2. Geochemical Characterization

3.2.1. CRM Abundance

The CRM abundance in EWs, kaolinitic gneisses, and soils after UCC standardization is shown in Figure 5a–d.

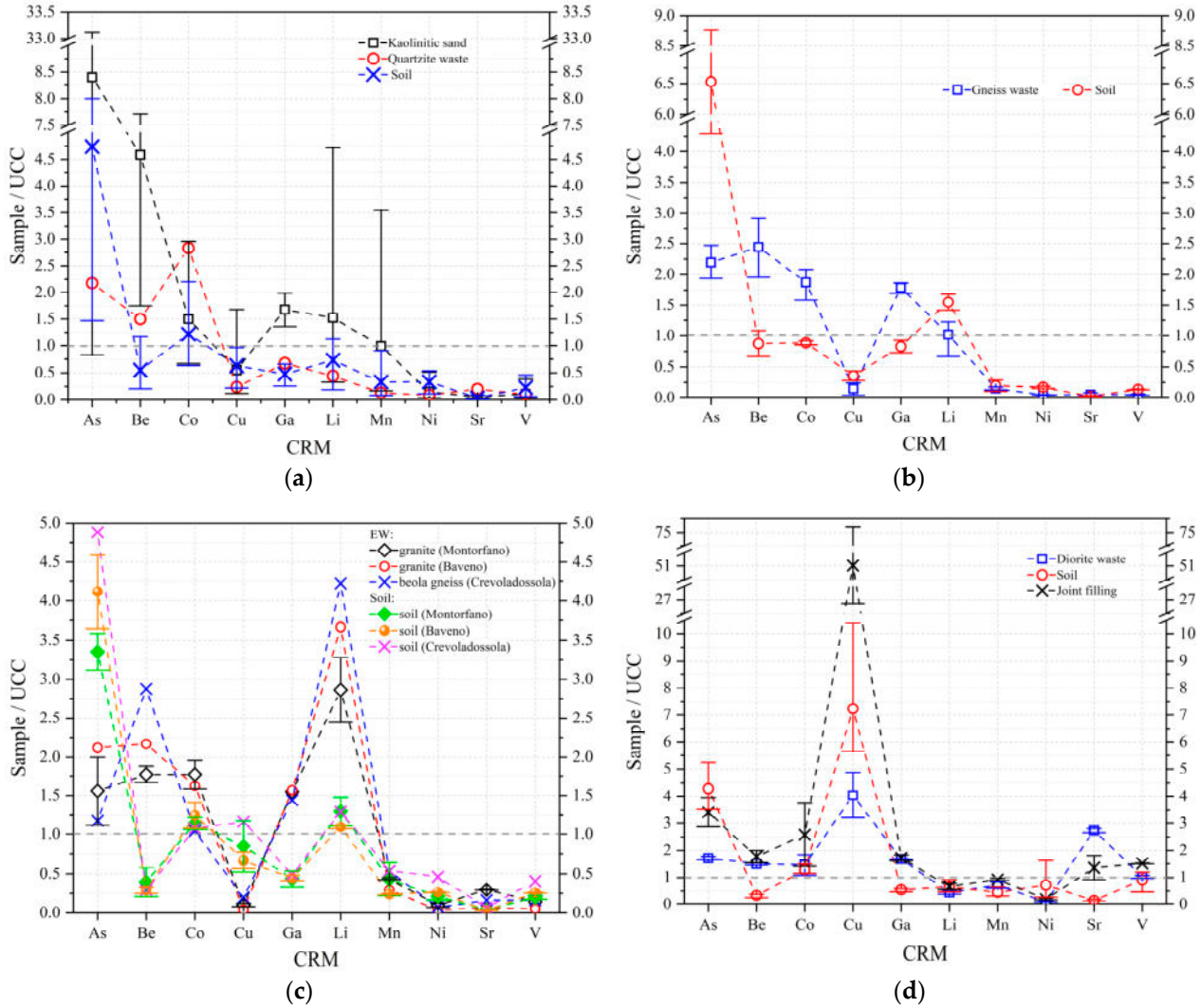

Figure 5. CRM abundance of EW, kaolinitic gneisses and soils from different areas: (**a**) Monte Bracco; (**b**) Luserna; (**c**) VCO; (**d**) Traversella.

Almost all samples showed As enrichment, with abundances in soils from all areas ranging from three to eight times higher than the UCC values, while lower concentrations were found in EWs. Except for the depletion of Ga in quartzite EW samples and Co in some kaolinitic gneisses samples from Monte Bracco, Be, Co, and Ga in EWs showed a noticeable enrichment.

In the Monte Bracco area, the abundance of As, Be, Li, Co, Cu, Ga, and Mn in brown kaolinitic gneiss sample R16 are significantly high. The concentrations of As, Be, Li, and Mn are 33 times, 7.7 times, 4.7 times, and 3.5 times higher than those of UCC, respectively. This may be attributed to the fact that the sample was taken from brown sand covered by white kaolinitic sand, and elemental ions migrate downward and accumulate under conditions such as precipitation and weathering [36,37]. Co in soil samples also shows significant enrichment. In the Luserna Stone quarry basin, Li is significantly enriched in the soil samples. In the VCO area, the CRM distribution pattern in granite waste samples from different sampling sites showed a high degree of consistency, as did the soil. Li, Co, and Cu in granite waste from Montorfano and Baveno show an enrichment, in which the abundance of Li generally exceeds 2.5 times the UCC values. In addition, the Mn content of R4, R5, and R9 is between 1050 and 1130 ppm, which is significantly higher than other samples with the same lithology from the same sampling area, such as R3 (108 ppm) and R8 (296 ppm). The high contents of Mn and Li in the samples could be attributed to the magnetic separation process during EW processing [38]. In the previously mentioned areas, Mn, Ni, Sr, and V in EWs with different lithologies and soils generally show significant depletion. In the Traversella area, Ga and Sr show an enrichment trend in diorite waste and joint filling, while Li, Mn, and Ni show depletion characteristics. As, Be, Co, and Cu are highly enriched in joint filling compared to diorite waste. For instance, Cu is 26–75 times more highly enriched than the UCC concentration and 3–5 times more highly enriched than that of diorite waste. Cu in soil also shows a significant enrichment. It is speculated that the joint filling contains soil components, which favor the precipitation of Cu.

3.2.2. REEs Abundance

The REEs abundance in EWs, kaolinitic gneisses, and soils after UCC normalization is shown in Figure 6a–d.

In Monte Bracco, heavy rare earth elements (HREEs) in kaolinitic gneiss (such as sample R14–16) generally show significant enrichment characteristics. In particular, the abundance of Tb, Ho, Er, Tm, Yb, and Dy in R15 is 5.0–5.7 times that of UCC. In the Luserna Stone quarry basin, gneiss EW is basically consistent with the enrichment trend of REEs in soil and is highly similar to the enrichment trend of REEs in kaolinitic gneiss from Monte Bracco. Among them, the most significantly enriched REE is Dy, whose maximum abundance in gneiss EW and soil exceeds UCC by 4.2 times and 2.4 times. The REE enrichment trend in the soil from this quarrying area indicates its potential geochemical connection with the presence of gneiss from EW facilities and the bedrock. In the VCO area, all soil samples and EW samples from Crevoladossola generally show depletion characteristics of REEs. Granite EW samples from processing plants in Montorfano and Baveno areas show REEs enrichment, except for Sc and Eu in sample R9, collected in the Baveno processing plant (magnetic fraction); REEs concentrations are significantly higher than those of the same lithology and in other areas due to magnetic separation processing (REE minerals tend to concentrate in the magnetic fraction coming from mineral processing to obtain the non-magnetic fraction, rich in feldspar and quartz, for the ceramics industry). The same is true for samples R4 and R5 from the processing plant in Montorfano (magnetic concentrates, where the presence of monazite is recognizable). Interestingly, the EW from Montorfano (white granite) is more enriched in LREEs than the EW from Baveno (pink granite), which is more enriched in HREEs. The abundance of Sc and Eu in EWs and soil in the above three areas generally showed significant depletion characteristics. In Traversella, the patterns of REE abundance in diorite EW and joint filling are consistent and are similar

to the soil pattern, which may indicate the close origin connection between soil, diorite, and joint fillings [39,40].

In summary, large differences were present in REEs concentrations between soil and EW samples in the same sampling area, which may be attributed to differences in the sampling locations, vegetation present on the surface, or humus and soil composition [41,42], or may be related to the REE and accessory minerals content in the soil parent materials or the migration of elements under physical and chemical effects [43,44].

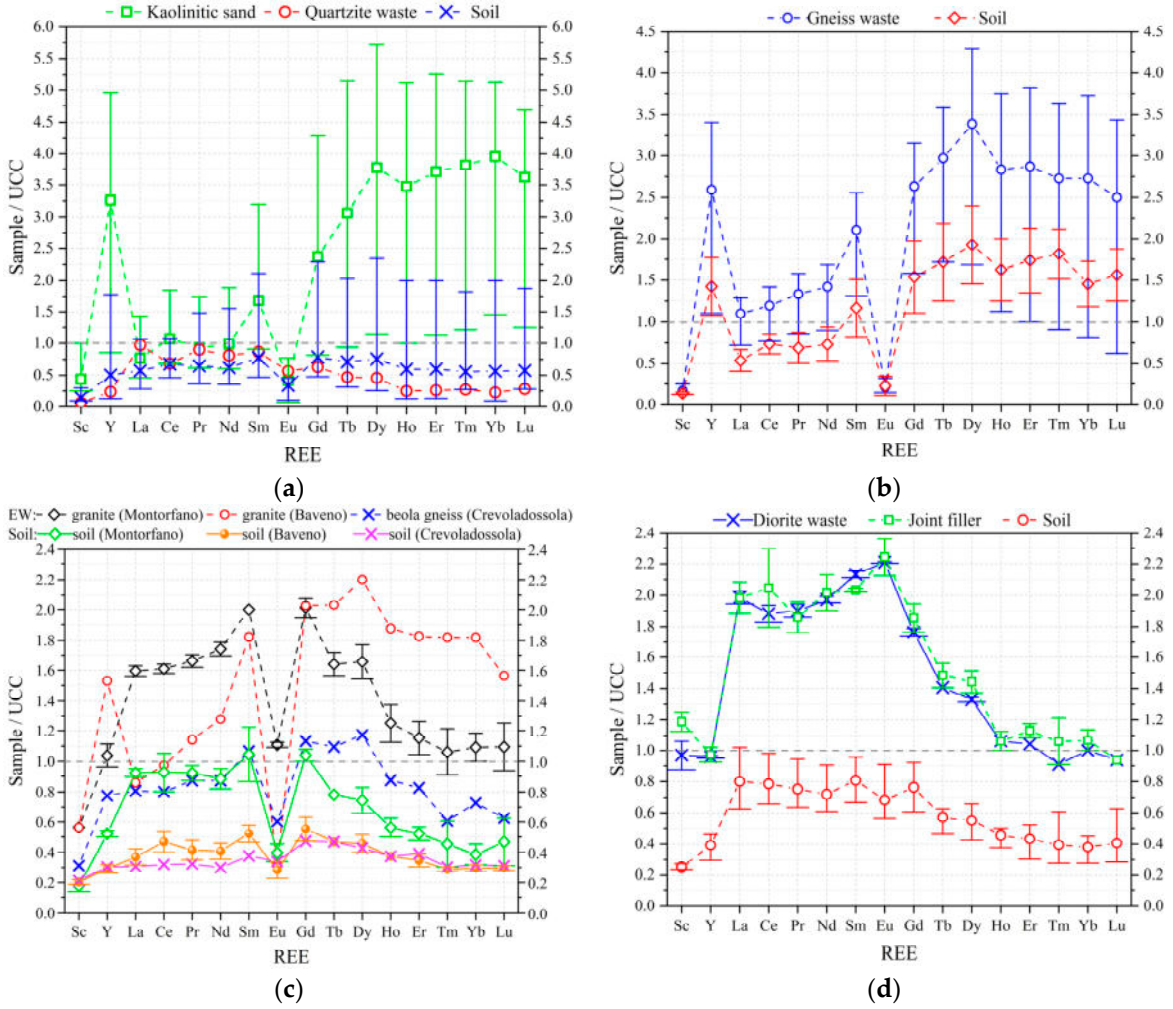

Figure 6. REEs abundance of EW, kaolinitic gneisses, and soils from different areas: (**a**) Monte Bracco; (**b**) Luserna; (**c**) VCO; (**d**) Traversella.

3.2.3. Geochemical characteristics

The geochemical characterization parameters of REEs for all samples are as shown in Figure 7.

In all sampling areas, the δEu of most samples is less than 0.8; the negative Eu anomaly is significant and may be related to complex geological movements or the evolution of feldspar mineral crystals [16,45]. The exception is sample R6, which has a positive δEu anomaly due to the enrichment of Eu during the magnetic separation of the samples in the processing plant. In the Luserna, Baveno, and Traversella areas, the δCe values of some EW and soil samples are greater than 1.2, showing positive anomalies in Ce. In Monte Bracco, most EW and soil samples show strong positive Ce anomalies, among which the maximum δCe value is 2.2 for kaolinitic sand sample R16. However, individual samples, such as R15 and R17 and soil MS10, show significant negative Ce anomalies. The drastic variations in

the Ce values of samples located in the same area might be caused by several natural factors, such as the weathering and pedogenesis of the rocks and soil or rock alteration [29,46].

The (La/Yb)N values of all samples are greater than 1. Their value in the soil is generally higher than those in EW, with a maximum value of 84 (MS6 Monte Bracco). This is translated into a right-skewed partitioning curve and an enrichment of LREEs. The (La/Sm)N and (Gd/Lu)N values of all samples basically fluctuate in the range of 1–5, and the changing trends show a high degree of consistency. The (La/Sm)N value is generally higher or comparable to the (Gd/Lu)N value. The highest (La/Sm)N value is found in the soil sample MS6 from the Monte Bracco area, indicating that this sample has the highest degree of fractionation of LREEs. The soil sample from Montorfano and the EW sample R20 from the Luserna area are the exceptions. The (La/Sm)N values of these samples are slightly smaller than the (Gd/Lu)N values, indicating that the degree of fractionation between HREEs is higher than that of LREEs.

With the exception of samples R12, R14, and R15, most of the EW samples and all soil samples had a ∑LREE/HREE value higher than 1 and 1.5, indicating a significant differentiation characteristic of LREE and HREE. The quartzite waste sample R17 from Monte Bracco has the greatest differentiation degree of LREEs and HREEs (∑LREE/HREE = 8.5).

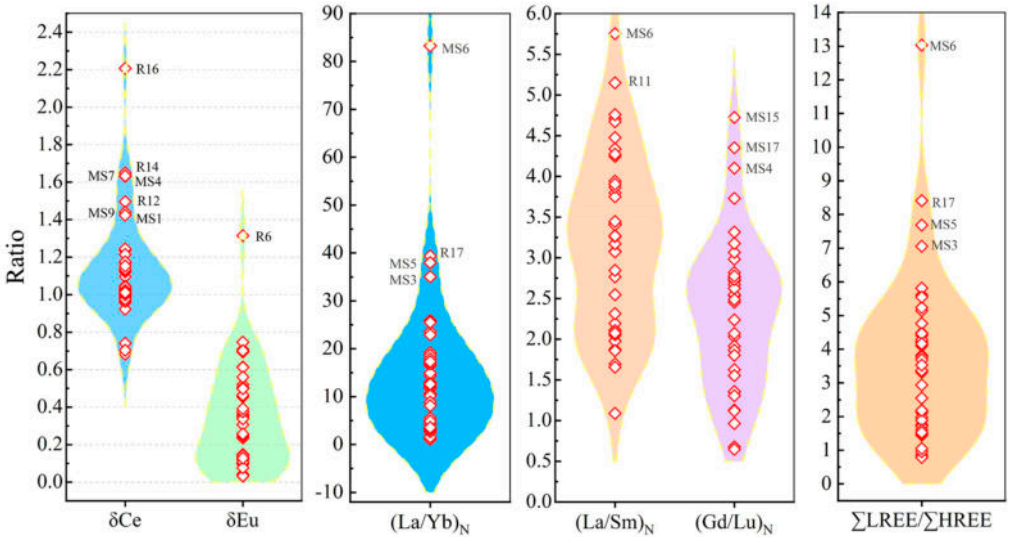

Figure 7. Geochemical characteristic parameters of REEs in all samples. The diamond shapes represent individual samples.

3.3. Environmental Risk

The concentration of potentially toxic elements (PTE) is shown in Tables A3 and A4 (Appendix A). The calculation results of the GI, PLI, EHC, and HI of soil heavy metals, as well as the EHC and HI of EW, are shown in Figure 8.

As shown in Tables A3 and A4, compared to samples from other sampling areas, both EW and soil from Traversella show high concentrations of Cu and Ba. In particular, the GI values of the soil samples from Traversella range from 1 to 3, indicating moderate Cu pollution [47]. It can be seen from the soil PLI that there is no regional contamination in the sampling area as a whole (PLI−zone < 1), but moderate contamination occurs in soil from the individual sampling site, such as MS19 from Traversella (PLI−site = 1.1). The ecological hazard risk of soil is generally low, but the EHC of Cu in soil samples from Traversella is relatively high. Among them, the EHC of Cu in the MS17 is as high as 52, showing a moderate ecological hazard risk [47]. The EHCs of Cd (concentration lower than the detection value) in most EW samples indicate low-to-moderate contamination. It should be noted that sample R16 has moderate-to-high ecological hazard risks of various PTE, such as Zn, Cd, and As, and EW samples R9 and R23 also have moderate ecological hazard risks of Cd and Cu, respectively. Human health risk assessment results indicate that the

non-carcinogenic and carcinogenic risks of all soil samples under three exposure pathways are negligible. Although the non-carcinogenic risks of EW samples are extremely low, some EW samples show unacceptable carcinogenic risks, such as R11 and R16 [48]. Overall, there are no regional environmental risks associated with soil and EW in the Luserna Stone basin, VCO, and Monte Bracco regions, but potential contamination risks of point-source or single PTE appear in soil and EW near the quarry, which may be related to external input and other factors. The soil and EW in Traversella are more challenging in terms of environmental risks compared to other areas, especially the regional risks brought by Cu, which may be related to local mining activities, as Traversella is also an important metal mining area in Piedmont.

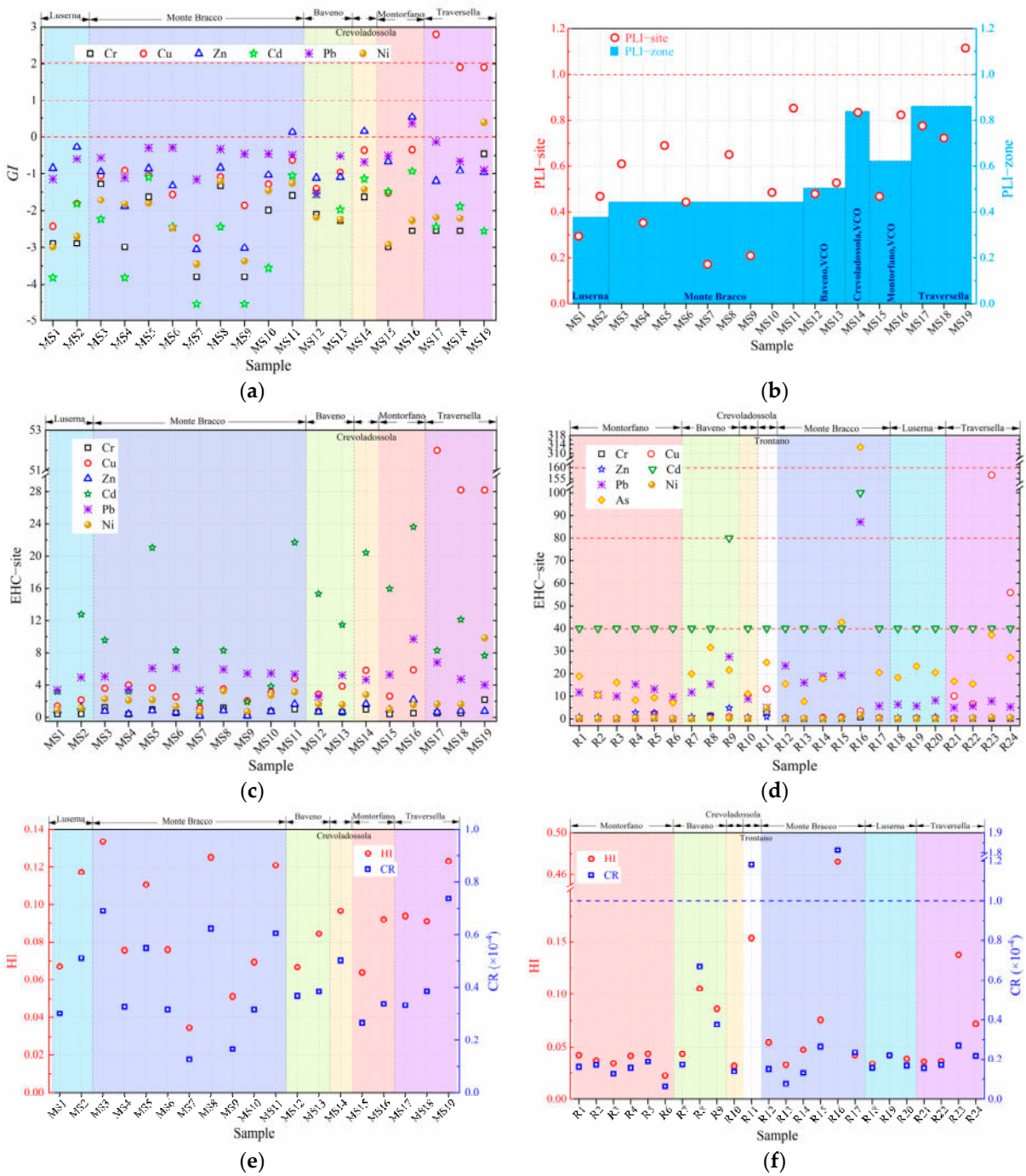

Figure 8. Potential environmental risks of soil and EW: (**a**) GI of soil; (**b**) PLI of soil; (**c**) EHC of soil; (**d**) EHC of EW; (**e**) human health risks of soil; (**f**) human health risks of EW.

4. REEs Recovery Potential of EW

4.1. Industrial Recovery Grade of REEs

Compared to soil, EW and kaolinitic gneiss from Monte Bracco showed a significant enrichment of REE. For this reason, EW samples were selected to be the subject of REEs potential recovery tests. Figure 9a shows the total content of REE, the content of critical REE, and the contents of HREEs. Figure 9b depicts the REEdef,rel–Coutl graph; REEdef,rel is the proportion of critical REEs in total REE, and Coutl is the outlook coefficient. Details of its calculation method and meaning can be found in the reference [49].

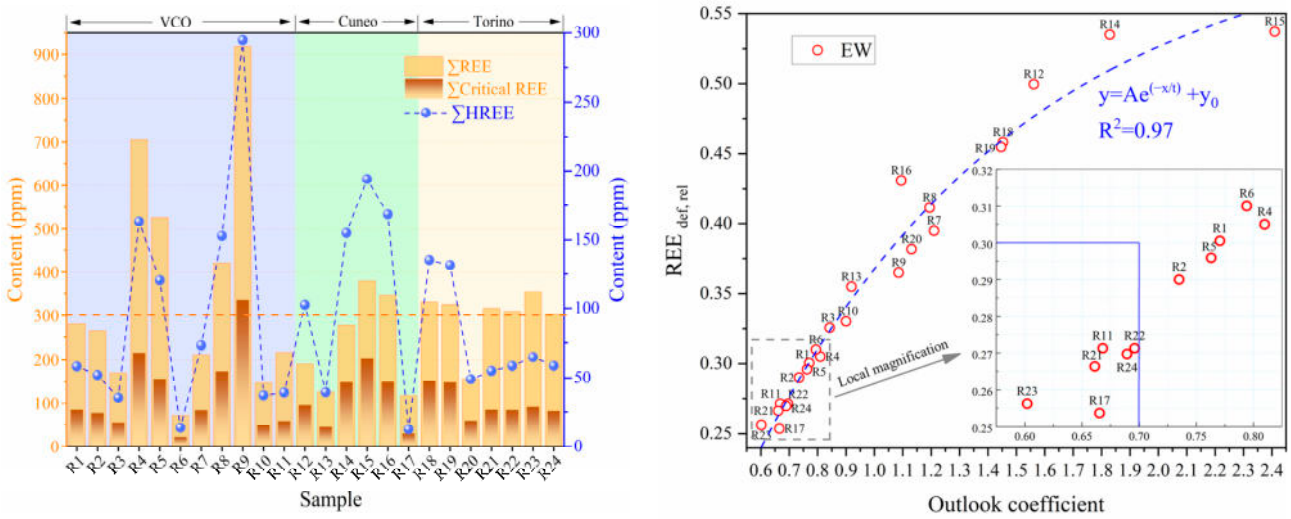

(**a**) (**b**)

Figure 9. Assessment of REEs industrial recovery potential: (**a**) contents of REEs with different classifications; (**b**) $REE_{def,rel}$ and outlook coefficient.

As displayed in Figure 9a, the total REEs concentration of the sample R9 from the processing plant in the Baveno area is the highest (919 ppm), followed by samples R4 and R5 from the processing plant in the Montorfano area. While sample R6 has the lowest REEs concentration at 71.4 ppm, samples R6 and R4 came from the same processing plant, but the REEs concentration differed by nearly 10 times, which is related to the magnetic separation processing of the sample (R6 is a non-magnetic concentrate for feldspar–quartz production for the ceramic industry and R4 is a magnetic concentrate arising from the processing plant; at present, it is used in civil and building applications).

It is generally believed that the minimum industrial grade necessary for the REEs recovery from a secondary resource is 300 ppm. Thus, such solid waste samples can have considerable economic benefits through REEs recovery [50,51]. In this study, there are a total of 12 groups of EW samples with REEs concentrations higher than 300 ppm. It is worth noting that the REEs concentrations of EW from Traversella are all higher than 300 ppm, showing regional characteristics.

Generally, EW with an outlook coefficient greater than 0.7 and a critical REEs accounting for more than 0.3 of the total REEs can be considered to have high industrial recovery potential [49,52]. As displayed in Figure 9b, the EW samples with Coutl under 0.7 and $REE_{def,rel}$ under 0.3 are diorite waste and joint filler samples R21–R24 from Traversella and the gneiss residual sludge sample R11 from Trontano. These five samples have low REEs industrial recovery potential; however, their REEs concentration is not low, ranging from 220 to 350 ppm. Other samples have outlook coefficients greater than 0.7 and REEdef,rel greater than 0.3, indicating high recovery potential. The samples with the greatest industrial recovery potential are kaolinitic sand samples R15 and R14 from Monte Bracco. Meanwhile, the critical REEs concentration and total REEs concentration in these two samples are not

the highest. The mathematical relationship between $REE_{def,rel}$ and Coutl, fitted to guide the assessment of REEs recovery potential in EW from Piedmont, Italy, is shown in Equation (1):

$$y = Ae^{(-x/t)} + y_0, \quad (1)$$

where y is $REE_{def,rel}$; x is Coutl; $y_0 = 0.61 \pm 0.03$; $A = -0.70 \pm 0.03$; $t = 0.95 \pm 0.16$.

4.2. Potential Market Value for REEs Recovery

Through the REE-recoverable amounts of each EW sample and the REEs market price, the potential market value for REEs recovery from EW is analyzed (Figure 10a). Assuming that the potential market value of each sample is the total market price P_total of REE recovered from the disposal of 1000 tons of EW, the calculation equation is as follows:

$$P_{total} = \sum k_{REE} c_w \times 10^6 \times p_{REE}, \quad (2)$$

where k_{REE} is the recovery rate of each REE in the waste. For the convenience of calculation, it is assumed in this study that the REEs recovery rate is 100%; c_w is the concentration of single REE in EW, mg/kg; $\sum k_{REE}\ c_w$ is the recoverable amount of REEs per kilogram of EW, mg; p_{REE} is the market price (CNY/kg) of each REE in the form of metal (except Eu in oxide form) before 30 November 2023 (as shown in Table A5, Appendix A).

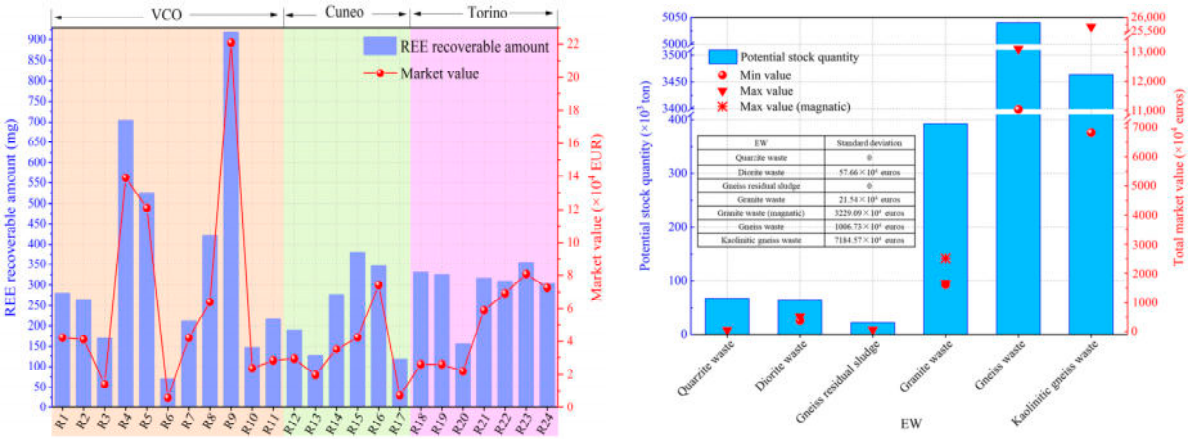

(**a**) (**b**)

Figure 10. Assessment of potential market revenue from REEs recovery: (**a**) potential market value of REE in each sample; (**b**) total market value and stock quantity of EW.

According to the Mining Activities Database of the Production Activities Directorate in the Piedmont region and published studies [23,53], a tentative evaluation of potential total stock quantity of the EW, corresponding to the investigated materials, was conducted (investigated period: 2005–2017). The total stock quantity of gneiss includes the stock quantity of Serizzo, Beola, and Pietra di Luserna. The waste production coefficient in the quarrying process is generally 0.4–0.8 [54,55]; a value of 0.4 is assumed in this study (considering the minimum waste production—potentially stored in EW facilities). The potential total market value (MVtotal) of waste with different lithologies is calculated based on stock quantity, as shown in Equation (3):

$$MV_{total} = W^a_{total} \times P^a_{REE}, \quad (3)$$

where W^a_{total} is the total stock quantity of EW with lithology a; and P^a_{REE} is the REEs market value (per kiloton) of EW with lithology al the maximum and minimum value of sample (including magnetic separation sample) with the corresponding lithologies were taken, respectively, in this study. The calculation results are shown in Figure 10b.

For our sites, an interesting positive association between the potential market value for REEs recovery and the REE-recoverable amounts in EW is visible (Figure 10a). For example, the REE recoverable amount in samples R4, R5, and R9 from the VCO area is significantly higher, and their potential market value is also high, exceeding 10×10^4 EUR. This highlights the economic effect of magnetic separation for REE recovery from EW. The lowest potential market values were found for sample R6 from the VCO area and R17 from the Monte Bracco are (below 1×10^4 EUR). Interestingly, the total REE recoverable amount of sample R17 is not significantly low; however, its potential market value for REE recovery is lower due to the lower concentrations of the more valuable HREEs.

Figure 10b demonstrates that there is a certain positive correlation between the total stock quantity of EW with different lithologies and its potential total market value of REE, indicating that the huge EW stock quantity is very conducive to the industrial recovery of REE. In the Piedmont region, the total stock quantity of quartzite waste, diorite waste, and gneiss residual sludge is less than 100×10^3 tons. If all the REE reserves in it are recovered, the potential maximum market value that can be obtained is near 1000×10^4 EUR. Magnetic separation can increase the total revenue of REE recovery. For example, after the magnetic separation of granite waste, its total potential market value of REE increased by nearly 1000×10^4 EUR. The total accumulated amount of gneiss waste and kaolinitic gneiss waste is estimated to be about (3500–5000) $\times 10^3$ tons in the period of 2005–2017; if all the REEs in EW are recovered, it is expected to have a potential market value of (7000–26,000) $\times 10^4$ EUR, which is a very considerable income for a company.

5. Challenges Facing REE Recovery

Despite the REE presence in gneiss and granite EWs in many areas, and the good REE industrial recovery prospects and potentials (Appendix B), several challenges still exist for future applications.

Potential environmental risk results show that the individual PTE concentration in some EWs may exceed the environmental standard limits for waste discharge and violate occupational labor environmental safety standards [42]. Samples with the highest REEs concentration and recovery market value—in particular, samples R9 and R16 from granite waste processing—have, paradoxically, higher ecological hazard and human carcinogenic risks. It has to be highlighted that the EWs, as such, do not cause environmental risks or risk for human safety in terms of metals (instead, issues connected to SiO_2 have to be faced in case of EW recovery and management, particularly for fine fractions), but such risks can be present in by-products (magnetic concentrate) produced during dressing activities. This positive and negative conflict will greatly hinder EW from carrying out large-scale REE recovery in a safe and environmentally friendly way. When carrying out REE recovery or other reuse work for these EW materials, it is necessary to take certain protective measures to reduce human health risks (particularly for workers) and contamination risks to the surrounding soil. All of these measures would undoubtedly increase the environmental protection cost of material disposal.

CRM and REEs in EWs from different sampling areas are unevenly distributed; even in the same sampling area, the concentrations of REEs could vary due to different lithologies. There are also significant differences in the REEs concentration of EWs from the same sampling area and the same lithology in the quarry (such as gneiss waste samples R20 and R19 in the Luserna area) due to the effects of metamorphism, weathering, alteration, accessory minerals, and other factors. For example, the kaolinitic sand samples R15 and R14 from the Monte Bracco area have very high REE recovery potential, whereas the REE recovery potential of the kaolinitic sand sample R13 within 50 m of the R15 sampling site is not significant, bringing certain difficulties to the efficient and large-scale industrial recovery. For EW with an REEs concentration below 300 ppm, not interesting for REE exploitation, a potential method for the collaborative recovery of REE and other CRMs or valuable metals can be used to improve the economic benefits of the recovery industry. The potential recovery method has already been stated in previous studies [56,57].

REEs recovery from waste also faces the problem of a mismatch between the potential market value and the annual waste production. The high REEs recovery potential is not only reflected in the high-grade of the waste but also in its high production [58,59]. The annual production of waste with different lithologies in the three provinces (the data refer to 2017) was compared with the potential market value of REE recovery for the collected samples, and the results are shown in Figure 11. Ref.$_{min}$, Ref.$_{max}$, and Ref.$_{ave}$, respectively, refer to the minimum, maximum, and average REEs concentration [15,23,25]. Equation (2) was used to calculate the potential market value of REEs recovery. Due to the lack of data on Sc and Y concentration in the literature, and based on the above-mentioned calculations of the potential market value of REE recovery for all EW samples, the potential recovery market value of Sc and Y in all samples was estimated for more than 50–70% of the total value. This study selects 60% for a conservative estimate.

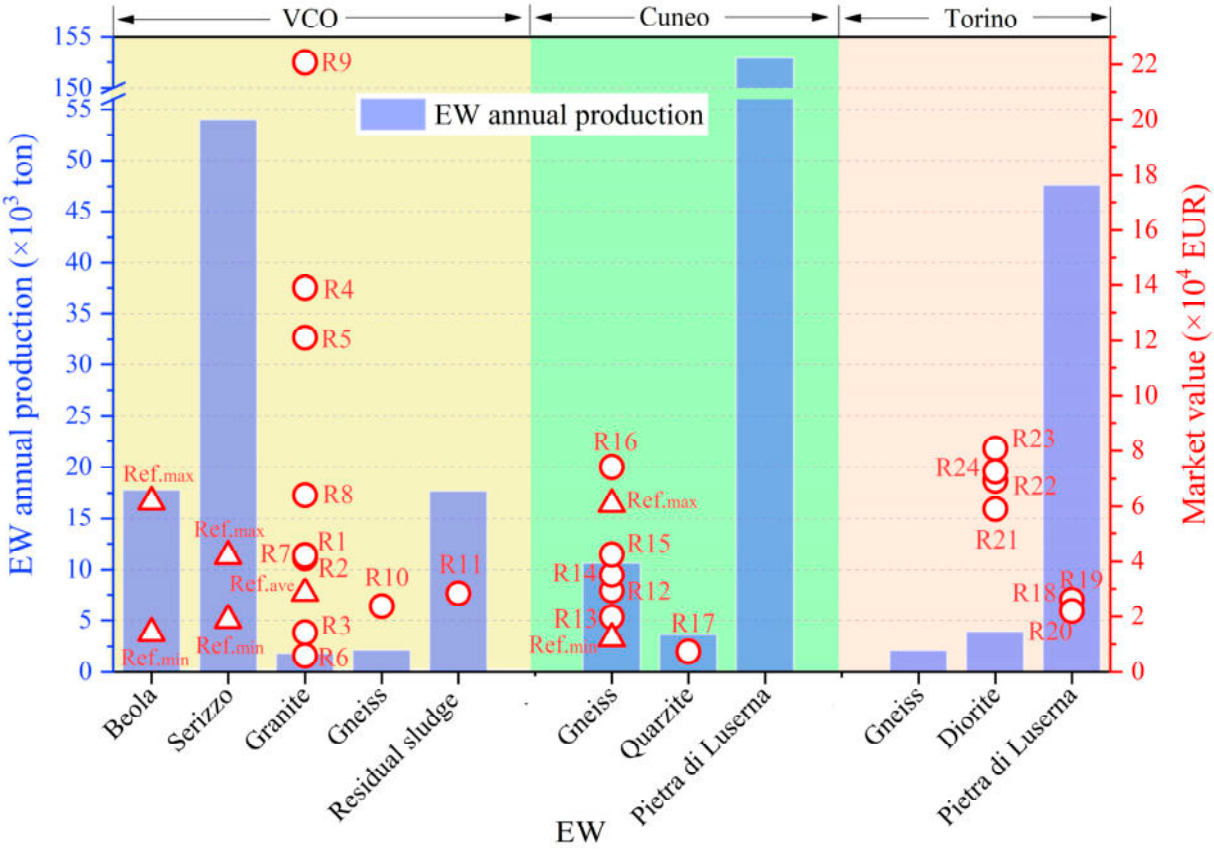

Figure 11. Potential REE recovery market value and EW annual production. The circles represent individual samples; the triangles show the Ref.$_{min}$, Ref.$_{max}$, and Ref.$_{ave}$, referred to the minimum, maximum, and average REEs concentration.

Samples with generally greater potential market value for REE recovery (Figure 11) are granite from Montorfano and Baveno (VCO area), diorite from Traversella (Turin Province), and brown kaolinitic gneiss from Monte Bracco (Cuneo Province). However, the annual production of these wastes results in a production that is insufficient to meet long-term sustainable REEs recovery on an industrial scale in a later stage (after EWs stock quantity is consumed). Although the annual production of EWs from Serizzo quarrying is significantly high, the maximum potential market value of its REEs recovery is less than 6.5×10^4 EUR. Similarly, with a high annual production, Pietra di Luserna has a low potential market value for REEs recovery.

At present, CRM and REEs recovery technology from waste is still at the laboratory stage (the potential REE recovery process is presented in Appendix C); the recovery

processes are usually lengthy with intensive chemical properties and low recovery efficiency [60]. Furthermore, the selective separation and purification of individual REEs is more challenging due to their chemical similarities [61]. The technology for large-scale recovery of REEs is not yet mature, and industrial application faces many challenges, such as cost, environment, and policy. A common problem in the hydrometallurgy process is the harmless treatment and safe reuse of a large amount of waste liquids and extraction solvents [62]. Large amounts of highly acidic waste liquids and solvents are more likely to cause environmental pollution, occupational hazards, and additional treatment costs. The use of pyrometallurgical processes to recover REEs from wastes faces the problem of high energy consumption and high carbon footprint [63]. Even with biohydrometallurgy, the efficiency of REEs recovery is not ideal [64]. If the economic benefits of recovered REEs cannot cover the operating costs, it could be difficult for companies to maintain operations in the long term without policy subsidies and financial support.

At present, various countries have no significant support for the technical application of REEs recovery from waste. Although the EU has proposed non-mandatory documents such as the Critical Raw Materials Act and the Circular Economy Action Plan, it has not invested sufficient subsidies to support companies in carrying out work on REEs recovery from EW. As the global supply of REEs has not yet experienced severe shortages, rare earth prices have not been extremely high, and REEs recovery from waste has not yet become mandatory, most companies have no incentive to recover REEs from waste [65,66].

6. Future Prospects

The results in this study provide a scientific basis for the recovery of EWs as resources and lay the foundation for the next research work.

Some EWs have potential environmental risks, but this requires comprehensive verification via the occurrence forms and leaching amounts of PTE, as well as the content of other pollutants. The next step is to analyze fractionation and mobility; in material with excessive pollutant leaching or strong migration, measures such as passivation, solidification, and adsorption can be taken to reduce risks.

REEs concentration in EW is related to the lithology, occurrence conditions, and location of the EW. The potential for REEs recovery from other quarry EWs is unknown due to the large variation of spatial REE abundance in the EW. A database showing the REEs concentration and recovery potential indicators of EWs from the whole Alps area could provide a scientific basis for the comprehensive assessment of the REEs recovery potential in the European region.

For EW samples rich in REEs and CRM, such as kaolinitic gneiss from Monte Bracco and granite from the Baveno processing plant, the next step should involve concentrating and extracting REEs. So far, few studies have been conducted on the extraction and recovery of REEs from gneiss and granite waste; the actual recovery rate is unknown, and the recovery process should be optimized by changing process parameters, reagent types, and extraction methods. Another determinant factor is the type and grade of ore minerals in the EW [67].

Some EWs with low abundance and recovery rates of REE, such as quartzite waste from Monte Bracco, could be of engineering and industrial use with respect to environmental protection, safety, and economic principles. For example, quartzite EW can be used as RM in the glass and ceramics industry [25], while granite or gneiss EW, when not processed to obtain feldspar–quartz concentrate for the ceramics industry, can be used in building materials [68]. The dumped EW in quarries could have adverse effects on the surrounding environment and landscape aesthetics and stability. These EWs with low REE recovery rates and low pollution risk can be used to backfill pits in abandoned quarries or can be mixed with soil and used for ecological restoration [69,70]. Furthermore, when mixed with natural soil and organic materials, EW could be transformed into an artificial substrate to promote site greening and to restore abandoned quarries [53].

7. Conclusions

Individual PTE in EWs from different sampling sites present varying degrees of potential environmental risks. EWs with different lithologies from the Monte Bracco, Luserna, and VCO areas generally show enrichment of As, Be, Co, and Ga. Be, Co, and Cu in diorite joint filling from Traversella are more enriched than diorite waste. HREEs in kaolinitic sand wastes from Monte Bracco generally show significant enrichment, which is very similar to the enrichment trend of REEs in gneiss wastes and soil from the Luserna Stone quarry. EW from Montorfano is richer in LREEs; whereas the EW from Baveno is richer in HREEs. Diorite wastes and joint fillings from Traversella show a prevalence of LREEs at the expense of HREEs. Geochemical characterization parameters of most samples show that the LREE fractionation is high, with significant differentiation of LREE and HREE.

This study proves that the REE recovery from EW is a promising topic. REEs concentration in half of the EW samples reaches industrial recovery grade, and most samples have good REE industrial recovery indicators. EW with high HREEs concentration also has a higher recovery rate. This trend is characteristic of gneiss and kaolinic gneiss wastes due to their huge total stock quantity. A potential and feasible process flowsheet for REE recovery from EW is developed, and REE recovery from EW is expected to achieve good laboratory and industrial effects.

However, REE recovery from EWs still faces some challenges in applications. Some EWs coming from processing activities pose ecological hazards and human health risks. REE abundance in EW is affected by factors such as weathering, alteration, parent rock, and minerals, and there are significant regional and lithological differences, which is not conducive to efficient and large-scale industrialization. The process of recovery could also be affected by the mismatch between the potential market value of REE recovery and the annual production of EW and the corresponding lithology in the later stage. Cost and policy challenges could be faced as well via the industrial application of existing technologies for REE recovery.

Author Contributions: Conceptualization, X.Z., F.K., M.C., A.C., E.P. and G.A.D.; methodology, X.Z., F.K., M.C., A.C., E.P. and G.A.D.; software, X.Z., F.K., M.C., A.C., E.P. and G.A.D.; validation, X.Z., A.C., E.P., K.Y. and G.A.D.; formal analysis, X.Z., F.K., M.C., A.C., E.P., K.Y. and G.A.D.; investigation, X.Z., F.K., M.C., A.C., E.P. and G.A.D.; resources, G.A.D.; data curation, X.Z., F.K., M.C., A.C., E.P. and G.A.D.; writing—original draft preparation, X.Z., F.K., M.C., A.C., E.P. and G.A.D.; writing—review and editing, X.Z., F.K., M.C., A.C., E.P. and G.A.D.; visualization, X.Z., F.K., M.C. and G.A.D.; supervision, X.Z., M.C., A.C., E.P. and G.A.D.; project administration, G.A.D.; funding acquisition, G.A.D. All authors have read and agreed to the published version of the manuscript.

Funding: This publication is part of the project NODES, which has received funding from the MUR—M4C2 1.5 of PNRR funded by the European Union—Next Generation EU (grant agreement no. ECS00000036). The authors wish to acknowledge the PRIN 2022 project EUREECA (2022Y4J7AN), and PhD research and training activities sponsored by the China Scholarship Council (CSC202208340044).

Data Availability Statement: The data used in this study are available upon request from the authors.

Acknowledgments: The authors wish to thank Antonio Tazzini and Marco Prati for their support during the laboratory activities.

Conflicts of Interest: The authors declare that they have no known competing financial interests or personal relationships that could have appeared to influence the work reported in this paper. The author Giovanna Antonella Dino is an Editorial Board Member for *Mining* (MDPI) and was not involved in the editorial review or the decision to publish this article; she is Topic Editor of the Special Issue "Sustainable Recycling and Reuse of Industrial By-Products or Waste from Geo-Resource Exploitation". The author Alessandro Cavallo is an Editorial Board Member and Guest Editor for *Sustainability* (MDPI) and was not involved in the editorial review or the decision to publish this article.

Appendix A

$$\delta Eu = \frac{2Eu_N}{Sm_N + Gd_N}, \tag{A1}$$

$$\delta Ce = \frac{2Ce_N}{La_N + Pr_N}, \tag{A2}$$

where Eu_N, Sm_N, Gd_N, Ce_N, La_N, and Pr_N are, respectively, the abundance values of each element after chondrite normalization.

$$GI = \log_2\left(\frac{C^i}{1.5C^i_{ref}}\right) \tag{A3}$$

$$PLI = \sqrt{\frac{C^1}{C^1_{ref}} \times \frac{C^2}{C^2_{ref}} \times \ldots \times \frac{C^i}{C^i_{ref}}} \tag{A4}$$

$$EHC^i = T^i \cdot \frac{C^i}{C^i_{ref}} \tag{A5}$$

$$ADD^i_{ing} = \frac{\mathrm{IngR} \cdot \mathrm{CF} \cdot \mathrm{EF_{ing}} \cdot \mathrm{ED_{ing}}}{\mathrm{BW} \cdot \mathrm{AT}} \cdot C^i \tag{A6}$$

$$ADD^i_{inh} = \frac{\mathrm{InhR} \cdot \mathrm{EF_{inh}} \cdot \mathrm{ED_{inh}}}{\mathrm{PEF} \cdot \mathrm{BW} \cdot \mathrm{AT}} \cdot C^i \tag{A7}$$

$$ADD^i_{derm} = \frac{\mathrm{SA} \cdot \mathrm{AF} \cdot \mathrm{ABS} \cdot \mathrm{CF} \cdot \mathrm{EF_{derm}} \cdot \mathrm{ED_{derm}}}{\mathrm{BW} \cdot \mathrm{AT}} \cdot C^i \tag{A8}$$

$$HI = \sum \frac{ADD^i}{RfD^i} \tag{A9}$$

$$CR = \sum ADD^i \times SF^i \tag{A10}$$

Table A1. Units, meanings, and values in equations [1–3].

Parameters	Unit	Meaning	Value
C^i	ppm	Concentration of element *i*	Tables A3 and A4
C^i_{ref}	ppm	Reference value of element *i*	Table A2
T^i	-	Toxic response coefficient for *i*	Table A2
ADD^i_{ing}	mg/(kg·d)	Average daily exposure doses of element *i* (ingestion)	-
ADD^i_{inh}	mg/(kg·d)	Average daily exposure doses of element *i* (inhalation)	-
ADD^i_{derm}	mg/(kg·d)	Average daily exposure doses of element *i* (dermal)	-
IngR	mg/d	Ingestion rate	100
$\mathrm{EF_{ing}} = \mathrm{EF_{inh}} = \mathrm{EF_{derm}}$	day/yr	Exposure frequency	250
$\mathrm{ED_{ing}} = \mathrm{ED_{inh}} = \mathrm{ED_{derm}}$	yr	Exposure duration	30
BW	kg	Body weight	60
AT	day	Average exposure time	7500
PEF	m^3/kg	Particle emission factor	1.36×10^9
InhR	m^3/d	Inhalation rate	20
CF	kg/mg	Conversion factor	0.000001
SA	cm^2	Exposed skin area	5700
AF	mg/cm^2	Skin adherence factor	0.07
ABS	-	Dermal absorption factor	0.001 0.03 (for As)
RfD^i	mg/(kg·d)	Reference dose of *i*	Table A2
SF^i	per mg/(kg·d)	Cancer slope factor of *i*	Table A2

Table A2. Value of various parameters for the different elements.

i	RfD^i Value (mg/(kg·d)) [2,4]			T^i Value [5]	SF^i Value (per mg/(kg·d)) [2,6,7]			C^i_{ref} Value (ppm) [8,9]	
	Ingestion	Inhalation	Dermal		Ingestion	Inhalation	Dermal	Soil	EW
Cr	0.003	0.0000286	0.00006	2	0.42	42	20	74	120
Cu	0.04	0.0402	0.012	5	-	-	-	25	60
Zn	0.3	0.3	0.06	1	-	-	-	69	70
Cd	0.001	0.00001	0.00001	30	6.1	6.3	20	0.47	0.15
Pb	0.0035	0.00352	0.000525	5	0.0085	0.042	-	42	14
Ni	0.02	0.00009	0.0054	5	-	0.84	-	46	84
As	0.0003	0.000123	0.000123	-	1.5	15.1	3.66	-	1.8

Table A3. Elemental content of potentially toxic elements in soil samples (ppm).

Sample	Cr	Cu	Zn	As	Cd	Pb	Ni	Ba
MS1	15	7	57.7	7.3	0.05	28.5	8.7	20.4
MS2	15	10.8	85.5	14.9	0.2	41.6	10.6	41.8
MS3	46	18	53.7	13.6	0.15	42.5	21	64.2
MS4	14	20	28	8.6	0.05	29.2	19.6	72.6
MS5	36	18.2	57.1	10	0.33	51.1	19.8	85.5
MS6	20	12.7	41.4	6.1	0.13	51.4	12.5	51.3
MS7	8	5.6	12.5	2.5	0.03	28.2	6.3	9.2
MS8	44	17.6	58.1	11.6	0.13	49.9	30.1	65.8
MS9	8	10.3	12.8	3.9	0.03	45.7	6.7	10.5
MS10	28	15.5	50.5	4.2	0.06	45.8	25.1	24.3
MS11	37	24.1	113	12	0.34	44.8	29	124
MS12	26	14.3	47.7	6.2	0.24	21.6	15.2	29.3
MS13	23	19.3	48.4	7.8	0.18	43.9	14.6	24.3
MS14	36	29.1	115	8.3	0.32	39.2	25.8	76.2
MS15	14	13.1	64.8	5.3	0.25	44.4	9.2	38
MS16	19	29.4	150	6.1	0.37	81.5	14.3	113
MS17	19	260	45.2	7	0.13	57.2	15.2	236
MS18	19	141	54.8	8.9	0.19	39.7	14.9	103
MS19	81	141	52.9	6	0.12	33.8	90.6	118

Table A4. Elemental content of potentially toxic elements in EW samples (ppm).

Sample	Cr	Cu	Zn	As	Cd	Pb	Ni	Ba
R1	7	3	65	3.4	0.2	33	7	435
R2	14	2	59	1.9	0.2	30	4	421
R3	4	2	20	2.9	0.2	28	4	333
R4	13	2	198	1.5	0.2	43	8	433
R5	17	29	187	1.7	0.2	37	8	439
R6	0.9	1	12	1.3	0.2	27	4	412
R7	8	1	66	3.6	0.2	33	2	75
R8	71	10	93	5.7	0.2	43	4	95
R9	32	12	340	3.9	0.4	77	4	89
R10	9	5	53	2	0.2	25	4	213
R11	149	159	67	4.5	0.2	14	83	453
R12	7	5	31	2.8	0.2	66	3	27
R13	2	3	15	1.4	0.2	45	4	104
R14	3	9	22	3.2	0.2	53	2	161
R15	6	10	35	7.7	0.2	54	4	379
R16	42	42	123	56.3	0.5	244	29	523
R17	17	6	28	3.7	0.2	16	5	644
R18	7	1	32	3.3	0.2	18	3	52
R19	13	4	30	4.2	0.2	16	2	44
R20	7	6	55	3.7	0.2	23	3	116
R21	8	122	25	3	0.2	14	4	1840
R22	11	80	33	2.8	0.2	16	6	2040
R23	11	1880	44	6.7	0.2	22	13	2050
R24	10	671	35	4.9	0.2	15	9	2150

Table A5. Market value of REEs.

REE	Price (EUR/kg)	REE	Price (EUR/kg)	REE	Price (EUR/kg)
La	3.21	Gd	31.41	Yb	12.82
Ce	3.33	Tb	1243.59	Lu	711.54
Pr	83.33	Dy	439.10	Sc	3461.54
Nd	78.21	Ho	70.51	Y	30.13
Sm	11.03	Er	36.28		
Eu_2O_3	25.00	Tm	500.00		

Appendix B. Potential REEs Recovery Process

Although there is currently no clear technical process route for REEs recovery from quarry EW, the REEs recovery process for solid wastes, such as mining tailings, can provide a reference. According to previous studies [71,72], a potential process flowsheet for REEs recovery from quarry EW is shown in Figure A1. This process route does not have any special technical difficulties, but it requires further verification and optimization of REE leaching parameters in the future.

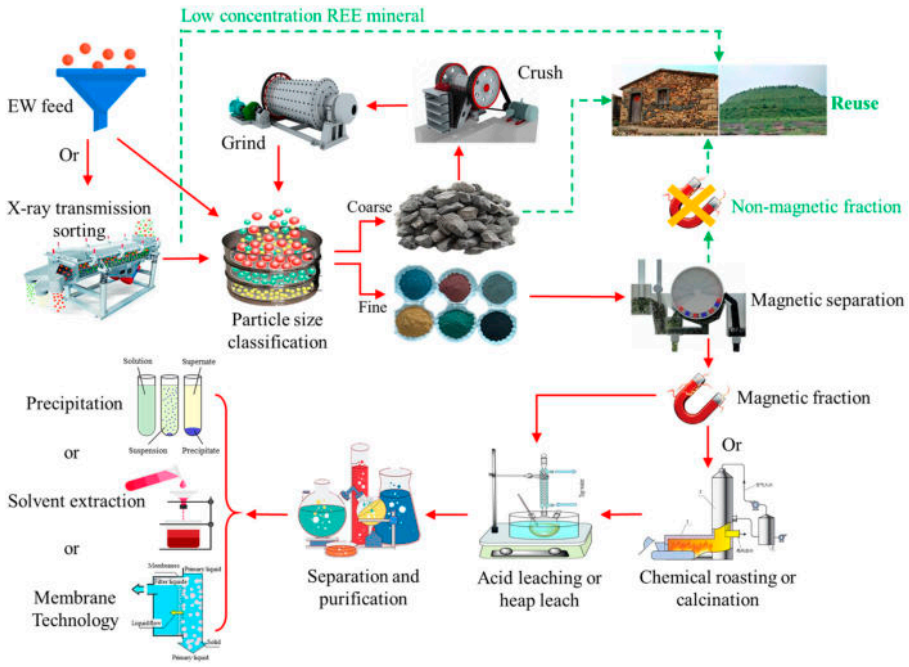

Figure A1. Potential flowsheet for REEs recovery from EW.

The potential process flowsheet of REEs recovery from quarry EW mainly includes steps such as classification, magnetic separation, leaching, separation, and purification. X-ray transmission sorting is an optional procedure before particle size classification, which can preliminarily sort out material with high concentrations of REEs [51]. Samples that are not sorted via X-ray transmission can be directly reused. Particle size classification consists of grinding EW into powder and sieving it into different particle sizes, such as 0.063 mm, 0.125 mm, and 0.25 mm, etc. Samples in the particle size range where REEs are enriched are used for the magnetic separation process. Samples in other particle size ranges can be ground again and reprocessed. Samples rich in REEs are magnetically separated at different magnetic susceptibilities to select the magnetic susceptibility that best enriches REEs to improve magnetic separation efficiency. Non-magnetic or weakly magnetic samples can be reused. The samples after magnetic separation are subjected to pre-treatment or leaching procedures. If economically feasible, EW can be chemically treated or calcined before leaching to improve REE leaching efficiency [73]. In the final stage, methods such as precipitation, solvent extraction, or membrane separation can be

used to separate and purify REEs [74]. The specific method needs to be selected based on the purification efficiency and recovery effect, as well as economic applicability.

Appendix C. Potential Recovery Rates

Due to the lack of research on REEs concentrations and recovery rates of dimension stones in Italy and the EU, the concentrations and recovery/extraction rates of REEs in different wastes from countries such as Portugal [75], Greece [76], Sweden [77], China [78–80], Tunisia [81], Brazil [82], the United States [83–86], Indonesia [87], and Canada [88,89] were collected and compared with EW samples with REEs concentrations higher than 300 ppm in this study to determine potential REEs recovery rates from EW (Figure A2). In these studies, different recovery or extraction methods (including different experimental conditions, parameters, reagents, equipment, etc.) were used, with results from 30 to nearly 100% recovery.

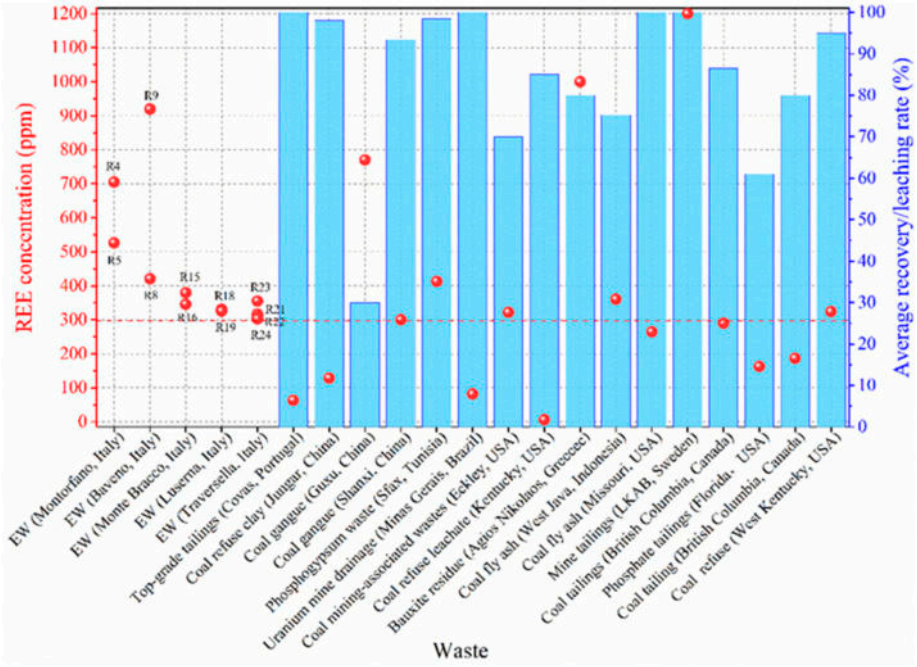

Figure A2. Comparison of EW in this study with waste from different countries and types. The circles represent individual samples.

Compared with the EW samples, REEs concentration in mining drainage and some coal-based and phosphate tailings is significantly lower than 300 ppm, but REEs recovery/extraction rates higher than 60–70% are generally still achieved at laboratory scale, providing the possibility for conducting a recovery experiment on EW with low REEs concentrations. It should be explained that coal gangue from the coal seam roof and floor (Guxu, China) contains a high REEs concentration (up to 770 ppm), but its REEs recovery/extraction rate is as low as 30%. This is attributed to the fact that the REEs in the sample mainly exist in the form of florencite, which hinders the leaching of REE. Fortunately, no significant presence of florencite mineral was found in the EW sample. Not only are the potential recovery/extraction rates generally significant, the industrial recovery of REEs in EW also has great potential to bring about circular economic benefits. Coal refuse from West Kentucky (USA) contains an REEs concentration of 324 ppm. Its pilot-scale REEs recovery trial shows that the return-on-investment period of REEs recovery is 5.5 years, the internal rate of return is 27%, and the economic benefits are considerable. Also, the higher the REEs concentration in the waste, the more industrial value REEs recovery has. This pilot trial provides a potential route to the economic recovery of REEs from wastes with REEs concentrations no lower than 300 ppm [51].

References

1. Yu, S.; Wu, S.C.; Dumont, L.; Cardin, J.; Labbé, C.; Gourbilleau, F. Monolithic crystalline silicon solar cells with SiNx layers doped with Tb3+ and Yb3+ rare-earth ions. *J. Rare Earths* **2019**, *37*, 515–519. [CrossRef]
2. Heier, S. *Grid Integration of Wind Energy: Onshore and Offshore Conversion Systems*; John Wiley & Sons: Hoboken, NJ, USA, 2014.
3. Nakamura, H. The current and future status of rare earth permanent magnets. *Scr. Mater.* **2018**, *154*, 273–276. [CrossRef]
4. Blengini, G.A.; Nuss, P.; Dewulf, J.; Nita, V.; Peirò, L.T.; Vidal-Legaz, B.; Latunussa, C.; Mancini, L.; Blagoeva, D.; Pennington, D.; et al. EU methodology for critical raw materials assessment: Policy needs and proposed solutions for incremental improvements. *Resour. Policy* **2017**, *53*, 12–19. [CrossRef]
5. Favot, M.; Massarutto, A. Rare-earth elements in the circular economy: The case of yttrium. *J. Environ. Manag.* **2019**, *240*, 504–510. [CrossRef]
6. Hartley, K.; Van Santen, R.; Kirchherr, J. Policies for transitioning towards a circular economy: Expectations from the European Union (EU). *Resour. Conserv. Recycl.* **2020**, *155*, 104634. [CrossRef]
7. Grohol, M.; Veeh, C.E.; Commission, I. *Directorate-General for Internal Market, Entrepreneurship, SMEs, Study on the Critical Raw Materials for the EU 2023—Final Report*; Publications Office of the European Union: Luxembourg, 2023.
8. Khelifi, F.; Mokadem, N.; Liu, G.; Yousaf, B.; Zhou, H.; Ncibi, K.; Hamed, Y. Occurrence, contamination evaluation and health risks of trace metals within soil, sediments and tailings in southern Tunisia. *Int. J. Environ. Sci. Technol.* **2022**, *19*, 6127–6140. [CrossRef]
9. Padoan, E.; Hernandez Kath, A.; Vahl, L.C.; Ajmone-Marsan, F. Potential Release of Zinc and Cadmium From Mine-Affected Soils Under Flooding, a Mesocosm Study. *Arch. Environ. Contam. Toxicol.* **2020**, *79*, 421–434. [CrossRef] [PubMed]
10. Zhao, X.; Yang, K.; Wei, Z.; He, X.; Chen, R. Study on the effect of multi-source solid waste on the performance of its backfill slurry. *Heliyon* **2023**, *9*, e16251. [CrossRef] [PubMed]
11. Zhao, X.; Yang, K.; Dino, G.A.; He, X.; Wei, Z.; Zhang, J. Feasibility and challenges of multi-source coal-based solid waste (CSW) for underground backfilling—A case study. *Process Saf. Environ. Prot.* **2024**, *181*, 8–25. [CrossRef]
12. Khelifi, F.; Melki, A.; Hamed, Y.; Adamo, P.; Caporale, A.G. Environmental and human health risk assessment of potentially toxic elements in soil, sediments, and ore-processing wastes from a mining area of southwestern Tunisia. *Environ. Geochem. Health* **2020**, *42*, 4125–4139. [CrossRef]
13. Khelifi, F.; Caporale, A.G.; Hamed, Y.; Adamo, P. Bioaccessibility of potentially toxic metals in soil, sediments and tailings from a north Africa phosphate-mining area: Insight into human health risk assessment. *J. Environ. Manag.* **2021**, *279*, 111634. [CrossRef]
14. Cavallo, A.; Dino, G.A. Quartz, feldspars and REE from gneiss waste materials: An example from the VCO province (Piedmont, northern Italy). In Proceedings of the EGU General Assembly 2022, Vienna, Austria, 23–27 May 2022. EGU22-3156. [CrossRef]
15. Cavallo, A.; Dino, G.A. Extractive Waste as a Resource: Quartz, Feldspars, and Rare Earth Elements from Gneiss Quarries of the Verbano-Cusio-Ossola Province (Piedmont, Northern Italy). *Sustainability* **2022**, *14*, 4536. [CrossRef]
16. Petrosino, P.; Sadeghi, M.; Albanese, S.; Andersson, M.; Lima, A.; De Vivo, B. REE contents in solid sample media and stream water from different geological contexts: Comparison between Italy and Sweden. *J. Geochem. Explor.* **2013**, *133*, 176–201. [CrossRef]
17. Hammache, Z.; Berbar, Y.; Bensaadi, S.; Trari, M.; Amara, M. Recovery of light rare earth elements by leaching and extraction from phosphate mining waste (Fluorapatite and Carbonate-Fluorapatite). *J. Afr. Earth Sci.* **2020**, *171*, 103937. [CrossRef]
18. Edahbi, M.; Plante, B.; Benzaazoua, M.; Pelletier, M. Geochemistry of rare earth elements within waste rocks from the Montviel carbonatite deposit, Québec, Canada. *Environ. Sci. Pollut. Res.* **2018**, *25*, 10997–11010. [CrossRef] [PubMed]
19. Costis, S.; Mueller, K.K.; Coudert, L.; Neculita, C.M.; Reynier, N.; Blais, J.F. Recovery potential of rare earth elements from mining and industrial residues: A review and cases studies. *J. Geochem. Explor.* **2021**, *221*, 106699. [CrossRef]
20. Cavallo, A.; Dino, G.A. The Bargiolina, a Striking Historical Stone from Monte Bracco (Piedmont, NW Italy) and a Possible Source of Industrial Minerals. *Sustainability* **2019**, *11*, 4293. [CrossRef]
21. Costa, E.; Dino, G.A.; Benna, P.; Rossetti, P. The Traversella Mining Site as Piemonte Geosite. *Geoheritage* **2019**, *11*, 55–70. [CrossRef]
22. Compagnoni, R.; Rolfo, F.; Groppo, C.; Hirajima, T.; Turello, R. Geological map of the ultra-high pressure Brossasco-Isasca unit (Western Alps, Italy). *J. Maps* **2012**, *8*, 465–472. [CrossRef]
23. Dino, G.A.; Cavallo, A.; Faraudello, A.; Rossi, P.; Mancini, S. Raw materials supply: Kaolin and quartz from ore deposits and recycling activities. The example of the Monte Bracco area (Piedmont, Northern Italy). *Resour. Policy* **2021**, *74*, 102413. [CrossRef]
24. Mehta, N.; Cocerva, T.; Cipullo, S.; Padoan, E.; Dino, G.A.; Ajmone-Marsan, F.; Cox, S.F.; Coulon, F.; De Luca, D.A. Linking oral bioaccessibility and solid phase distribution of potentially toxic elements in extractive waste and soil from an abandoned mine site: Case study in Campello Monti, NW Italy. *Sci. Total Environ.* **2019**, *651*, 2799–2810. [CrossRef] [PubMed]
25. Dino, G.A.; Cavallo, A.; Rossetti, P.; Garamvölgyi, E.; Sándor, R.; Coulon, F. Towards Sustainable Mining: Exploiting Raw Materials from Extractive Waste Facilities. *Sustainability* **2020**, *12*, 2383. [CrossRef]
26. Dino, G.A.; Rossetti, P.; Perotti, L.; Alberto, W.; Sarkka, H.; Coulon, F.; Wagland, S.; Griffiths, Z.; Rodeghiero, F. Landfill mining from extractive waste facilities: The importance of a correct site characterisation and evaluation of the potentialities. A case study from Italy. *Resour. Policy* **2018**, *59*, 50–61. [CrossRef]
27. Jiu, B.; Huang, W.; Hao, R. A method for judging depositional environment of coal reservoir based on coal facies parameters and rare earth element parameters. *J. Pet. Sci. Eng.* **2021**, *207*, 109128. [CrossRef]
28. Zhou, L.; Kang, Z.; Wang, Z.; Peng, Y.; Xiao, H. Sedimentary geochemical investigation for paleoenvironment of the Lower Cambrian Niutitang Formation shales in the Yangtze Platform. *J. Pet. Sci. Eng.* **2017**, *159*, 376–386. [CrossRef]

29. Shi, Y.; Peng CE, Q.; Zhang, Z.; Zhang, J.; Yan, W.; Xu, C. Rare earth elements in aeolian loess sediments from Menyuan Basin, northeastern Tibetan plateau: Implications for provenance. *Front. Environ. Sci.* **2023**, *11*, 1074909. [CrossRef]
30. Hakanson, L. An ecological risk index for aquatic pollution control.a sedimentological approach. *Water Res.* **1980**, *14*, 975–1001. [CrossRef]
31. Muller, G. Index of geoaccumulation in sediments of the Rhine river. *GeoJournal* **1969**, *2*, 108–118.
32. Mohammadi, A.A.; Zarei, A.; Majidi, S.; Ghaderpoury, A.; Hashempour, Y.; Saghi, M.H.; Alinejad, A.; Yousefi, M.; Hosseingholizadeh, N.; Ghaderpoori, M. Carcinogenic and non-carcinogenic health risk assessment of heavy metals in drinking water of Khorramabad, Iran. *MethodsX* **2019**, *6*, 1642–1651. [CrossRef]
33. Fabietti, G.; Biasioli, M.; Barberis, R.; Ajmone-Marsan, F. Soil contamination by organic and inorganic pollutants at the regional scale: The case of Piedmont, Italy. *J. Soils Sediments* **2010**, *10*, 290–300.
34. Wedepohl, K.H. The composition of the continental crust. *Geochim. Cosmochim. Acta* **1995**, *59*, 1217–1232. [CrossRef]
35. Borst, A.M.; Smith, M.P.; Finch, A.A.; Estrade, G.; Villanova-de-Benavent, C.; Nason, P.; Marquis, E.; Horsburgh, N.J.; Goodenough, K.M.; Xu, C.; et al. Adsorption of rare earth elements in regolith-hosted clay deposits. *Nat. Commun.* **2020**, *11*, 4386. [CrossRef]
36. Zhang, X.; Yang, H.; Cui, Z. Evaluation and analysis of soil migration and distribution characteristics of heavy metals in iron tailings. *J. Clean. Prod.* **2018**, *172*, 475–480. [CrossRef]
37. Ye, Y.; Li, Y.; Cao, Z.; Liu, S.; Zhao, Y. Experimental and numerical study on Cu and Cd migration in different functional-area soils under simulated rainfall conditions. *Environ. Res.* **2022**, *208*, 112239. [CrossRef]
38. Dutta, T.; Kim, K.H.; Uchimiya, M.; Kwon, E.E.; Jeon, B.H.; Deep, A.; Yun, S.T. Global demand for rare earth resources and strategies for green mining. *Environ. Res.* **2016**, *150*, 182–190. [CrossRef]
39. Buss, H.L.; Sak, P.B.; Webb, S.M.; Brantley, S.L. Weathering of the Rio Blanco quartz diorite, Luquillo Mountains, Puerto Rico: Coupling oxidation, dissolution, and fracturing. *Geochim. Cosmochim. Acta* **2008**, *72*, 4488–4507. [CrossRef]
40. Tazikeh, H.; Khormali, F.; Amini, A.; Motlagh, M.B. Geochemistry of soils derived from selected sedimentary parent rocks in Kopet Dagh, North East Iran. *J. Geochem. Explor.* **2018**, *194*, 52–70. [CrossRef]
41. Hu, Z.; Haneklaus, S.; Sparovek, G.; Schnug, E. Rare Earth Elements in Soils. *Commun. Soil Sci. Plant Anal.* **2006**, *37*, 1381–1420. [CrossRef]
42. Li, W.; Zuo, Y.; Wang, L.; Wan, X.; Yang, J.; Liang, T.; Song, H.; Weihrauch, C.; Rinklebe, J. Abundance, spatial variation, and sources of rare earth elements in soils around ion-adsorbed rare earth mining areas. *Environ. Pollut.* **2022**, *313*, 120099. [CrossRef]
43. He, Y.; Ma, L.; Li, X.; Wang, H.; Liang, X.; Zhu, J.; He, H. Mobilization and fractionation of rare earth elements during experimental bio-weathering of granites. *Geochim. Cosmochim. Acta* **2023**, *343*, 384–395. [CrossRef]
44. Liang, T.; Li, K.; Wang, L. State of rare earth elements in different environmental components in mining areas of China. *Environ. Monit. Assess.* **2014**, *186*, 1499–1513. [CrossRef]
45. Relvini, A.; Martin, S.; Carvalho, B.B.; Prosser, G.; Toffolo, L.; Macera, P.; Bartoli, O. Genesis of the Eastern Adamello Plutons (Northern Italy): Inferences for the Alpine Geodynamics. *Geosciences* **2022**, *12*, 13. [CrossRef]
46. Skurzyński, J.; Jary, Z.; Kenis, P.; Kubik, R.; Moska, P.; Raczyk, J.; Seul, C. Geochemistry and mineralogy of the Late Pleistocene loess-palaeosol sequence in Złota (near Sandomierz, Poland): Implications for weathering, sedimentary recycling and provenance. *Geoderma* **2020**, *375*, 114459. [CrossRef]
47. Gujre, N.; Mitra, S.; Soni, A.; Agnihotri, R.; Rangan, L.; Rene, E.R.; Sharma, M.P. Speciation, contamination, ecological and human health risks assessment of heavy metals in soils dumped with municipal solid wastes. *Chemosphere* **2021**, *262*, 128013. [CrossRef]
48. Tume, P.; González, E.; King, R.W.; Monsalve, V.; Roca, N.; Bech, J. Spatial distribution of potentially harmful elements in urban soils, city of Talcahuano, Chile. *J. Geochem. Explor.* **2018**, *184*, 333–344. [CrossRef]
49. Seredin, V.V. A new method for primary evaluation of the outlook for rare earth element ores. *Geol. Ore Depos.* **2010**, *52*, 428–433. [CrossRef]
50. Sun, Y.; Zhao, C.; Li, Y.; Wang, J. Minimum mining grade of the selected trace elements in Chinese coal. *J. China Coal Soc.* **2014**, *39*, 744–748.
51. Honaker, R.Q.; Zhang, W.; Werner, J.; Noble, A.; Luttrell, G.H.; Yoon, R.H. Enhancement of a Process Flowsheet for Recovering and Concentrating Critical Materials from Bituminous Coal Sources, Mining. *Metall. Explor.* **2020**, *37*, 3–20.
52. Seredin, V.V.; Dai, S. Coal deposits as potential alternative sources for lanthanides and yttrium. *Int. J. Coal Geol.* **2012**, *94*, 67–93. [CrossRef]
53. Zichella, L.; Dino, G.A.; Bellopede, R.; Marini, P.; Padoan, E.; Passarella, I. Environmental impacts, management and potential recovery of residual sludge from the stone industry: The piedmont case. *Resour. Policy* **2020**, *65*, 101562. [CrossRef]
54. Mendoza, J.-M.F.; Feced, M.; Feijoo, G.; Josa, A.; Gabarrell, X.; Rieradevall, J. Life cycle inventory analysis of granite production from cradle to gate. *Int. J. Life Cycle Assess.* **2014**, *19*, 153–165. [CrossRef]
55. Ulubeyli, G.C.; Artir, R. Properties of Hardened Concrete Produced by Waste Marble Powder. *Procedia-Soc. Behav. Sci.* **2015**, *195*, 2181–2190. [CrossRef]
56. Borra, C.R.; Blanpain, B.; Pontikes, Y.; Binnemans, K.; Van Gerven, T. Recovery of Rare Earths and Other Valuable Metals from Bauxite Residue (Red Mud): A Review. *J. Sustain. Metall.* **2016**, *2*, 365–386. [CrossRef]
57. Zhang, W.; Honaker, R. Characterization and recovery of rare earth elements and other critical metals (Co, Cr, Li, Mn, Sr, and V) from the calcination products of a coal refuse sample. *Fuel* **2020**, *267*, 117236. [CrossRef]

58. Gaustad, G.; Williams, E.; Leader, A. Rare earth metals from secondary sources: Review of potential supply from waste and byproducts, Resources. *Conserv. Recycl.* **2021**, *167*, 105213. [CrossRef]
59. Mancini, S.; Casale, M.; Rossi, P.; Faraudello, A.; Dino, G.A. Operative instruments to support public authorities and industries for the supply of raw materials: A decision support tool to evaluate the sustainable exploitation of extractive waste facilities. *Resour. Policy* **2023**, *81*, 103338. [CrossRef]
60. Deng, B.; Wang, X.; Luong, D.X.; Carter, R.A.; Wang, Z.; Tomson, M.B.; Tour, J.M. Rare earth elements from waste. *Sci. Adv.* **2022**, *8*, eabm3132. [CrossRef]
61. Balaram, V. Rare earth elements: A review of applications, occurrence, exploration, analysis, recycling, and environmental impact. *Geosci. Front.* **2019**, *10*, 1285–1303. [CrossRef]
62. Peelman, S.; Sun ZH, I.; Sietsma, J.; Yang, Y. Chapter 21—Leaching of Rare Earth Elements: Review of Past and Present Technologies. In *Rare Earths Industry*; De Lima, I.B., Leal, W.F., Eds.; Elsevier: Boston, MA, USA, 2016; pp. 319–334.
63. Polyakov, E.G.; Sibilev, A.S. Recycling Rare-Earth-Metal Wastes by Pyrometallurgical Methods. *Metallurgist* **2015**, *59*, 368–373. [CrossRef]
64. Swain, B. Challenges and opportunities for sustainable valorization of rare earth metals from anthropogenic waste. *Rev. Environ. Sci. Bio/Technol.* **2023**, *22*, 133–173. [CrossRef]
65. Ambaye, T.G.; Vaccari, M.; Castro, F.D.; Prasad, S.; Rtimi, S. Emerging technologies for the recovery of rare earth elements (REEs) from the end-of-life electronic wastes: A review on progress, challenges, and perspectives. *Environ. Sci. Pollut. Res.* **2020**, *27*, 36052–36074. [CrossRef]
66. Royen, H.; Fortkamp, U. *Rare Earth Elements—Purification, Separation and Recycling*; IVL Svenska Miljöinstitutet: Stockholm, Sweden, 2016.
67. Kuppusamy, V.K.; Holuszko, M. Sulfuric acid baking and water leaching of rare earth elements from coal tailings. *Fuel* **2022**, *319*, 123738. [CrossRef]
68. Fasana, S.; Nelva, R. Improvement of the performance of traditional stone roofs by wind driven rain experimental tests. *Constr. Build. Mater.* **2011**, *25*, 1491–1502. [CrossRef]
69. Yang, K.; Zhao, X.; Wei, Z.; Zhang, J. Development overview of paste backfill technology in China's coal mines: A review. *Environ. Sci. Pollut. Res.* **2021**, *28*, 67957–67969. [CrossRef]
70. Zhao, X.; Yang, K.; Li, X.; Cheng, L. The Material Mix Proportion of Roadside Backfill Body (RBB) Based on Spatiotemporal Law of Ground Pressure: A Case Study. *Energy Explor. Exploit.* **2023**, *42*, 01445987231190786. [CrossRef]
71. Zhang, W.; Honaker, R. Calcination pretreatment effects on acid leaching characteristics of rare earth elements from middlings and coarse refuse material associated with a bituminous coal source. *Fuel* **2019**, *249*, 130–145. [CrossRef]
72. Ji, B.; Li, Q.; Zhang, W. Leaching recovery of rare earth elements from the calcination product of a coal coarse refuse using organic acids. *J. Rare Earths* **2022**, *40*, 318–327. [CrossRef]
73. Taggart, R.K.; Hower, J.C.; Hsu-Kim, H. Effects of roasting additives and leaching parameters on the extraction of rare earth elements from coal fly ash. *Int. J. Coal Geol.* **2018**, *196*, 106–114. [CrossRef]
74. Pan, J.; Nie, T.; Vaziri Hassas, B.; Rezaee, M.; Wen, Z.; Zhou, C. Recovery of rare earth elements from coal fly ash by integrated physical separation and acid leaching. *Chemosphere* **2020**, *248*, 126112. [CrossRef]
75. Tunsu, C.; Menard, Y.; Eriksen, D.O.; Ekberg, C.; Petranikova, M. Recovery of critical materials from mine tailings: A comparative study of the solvent extraction of rare earths using acidic, solvating and mixed extractant systems. *J. Clean. Prod.* **2019**, *218*, 425–437. [CrossRef]
76. Borra, C.R.; Pontikes, Y.; Binnemans, K.; Van Gerven, T. Leaching of rare earths from bauxite residue (red mud). *Miner. Eng.* **2015**, *76*, 20–27. [CrossRef]
77. Peelman, S.; Kooijman, D.; Sietsma, J.; Yang, Y. Hydrometallurgical Recovery of Rare Earth Elements from Mine Tailings and WEEE. *J. Sustain. Metall.* **2018**, *4*, 367–377. [CrossRef]
78. Pan, J.; Nie, T.; Zhou, C.; Yang, F.; Jia, R.; Zhang, L.; Liu, H. The effect of calcination on the occurrence and leaching of rare earth elements in coal refuse. *J. Environ. Chem. Eng.* **2022**, *10*, 108355. [CrossRef]
79. Zhang, W.; Noble, A. Mineralogy characterization and recovery of rare earth elements from the roof and floor materials of the Guxu coalfield. *Fuel* **2020**, *270*, 117533. [CrossRef]
80. Wu, H.; Yang, J.; Huang, L.; Huang, W.; Duan, S.; Ji, S.; Zhang, G.; Ma, J.; Deng, J. Full-components utilization: Study on simultaneous preparation of sodalite and separation of yttrium from coal gangue by chlorination roasting process. *Sep. Purif. Technol.* **2024**, *332*, 125802. [CrossRef]
81. Masmoudi-Soussi, A.; Hammas-Nasri, I.; Horchani-Naifer, K.; Férid, M. Rare earths recovery by fractional precipitation from a sulfuric leach liquor obtained after phosphogypsum processing. *Hydrometallurgy* **2020**, *191*, 105253. [CrossRef]
82. Moraes ML, B.; Murciego, A.; Álvarez-Ayuso, E.; Ladeira AC, Q. The role of Al13-polymers in the recovery of rare earth elements from acid mine drainage through pH neutralization. *Appl. Geochem.* **2020**, *113*, 104466. [CrossRef]
83. Yang, X.; Rozelle, P.L.; Pisupati, S.V. The effect of caustic soda treatment to recover rare earth elements from secondary feedstocks with low concentrations. *Miner. Eng.* **2021**, *173*, 107184. [CrossRef]
84. Zhang, W.; Honaker, R.Q. Rare earth elements recovery using staged precipitation from a leachate generated from coarse coal refuse. *Int. J. Coal Geol.* **2018**, *195*, 189–199. [CrossRef]

85. King, J.F.; Taggart, R.K.; Smith, R.C.; Hower, J.C.; Hsu-Kim, H. Aqueous acid and alkaline extraction of rare earth elements from coal combustion ash. *Int. J. Coal Geol.* **2018**, *195*, 75–83. [CrossRef]
86. Liang, H.; Zhang, P.; Jin, Z.; De Paoli, D.W. Rare Earth and Phosphorus Leaching from a Flotation Tailings of Florida Phosphate Rock. *Minerals* **2018**, *8*, 416. [CrossRef]
87. Rosita, W.; Bendiyasa, I.M.; Perdana, I.; Anggara, F. Recovery of rare earth elements and Yttrium from Indonesia coal fly ash using sulphuric acid leaching. *AIP Conf. Proc.* **2020**, *2223*, 050004.
88. Kuppusamy, V.K.; Kumar, A.; Holuszko, M.E. Simultaneous Extraction of Clean Coal and Rare Earth Elements From Coal Tailings Using Alkali-Acid Leaching Process. *J. Energy Resour. Technol.* **2019**, *141*, 070708. [CrossRef]
89. Li, X.; Jiang, R.; Wang, G.; Chen, Y.; Long, T.; Lin, Y. A Comparative Study of Soil Environmental Standards for Agricultural Land Among Different Countries and Its Implication for China. *Environ. Sci.* **2022**, *43*, 577–585.